MILIMETERWAVE FMCW RADAR DESIGN

A THESIS SUBMITTED TO
THE GRADUATE SCHOOL OF NATURAL AND APPLIED SCIENCES
OF
MIDDLE EAST TECHNICAL UNIVERSITY

BY

DİLŞAD İÇÖZ

IN PARTIAL FULFILLMENT OF THE REQUIREMENTS
FOR
THE DEGREE OF MASTER OF SCIENCE
IN
ELECTRICAL AND ELECTRONICS ENGINEERING

DECEMBER 2009

Approval of the thesis:

MILIMETERWAVE FMCW RADAR DESIGN

submitted by **DİLŞAD İÇÖZ** in partial fulfillment of the requirements for the degree of **Master of Science in Electrical and Electronics Engineering Department, Middle East Technical University** by,

Prof. Dr. Canan Özgen
Dean, Graduate School of **Natural and Applied Sciences** _____

Prof. Dr. İsmet Erkmen
Head of Department, **Electrical and Electronics Engineering** _____

Prof. Dr. Altunkan Hızal
Supervisor, **Electrical and Electronics Eng. Dept., METU** _____

Assoc. Prof. Dr. Şimşek Demir
Co-Supervisor, **Electrical and Electronics Eng. Dept., METU** _____

Examining Committee Members:

Prof. Dr. Murat Aşkar
Electrical and Electronics Engineering Dept., METU _____

Prof. Dr. Altunkan Hızal
Electrical and Electronics Engineering Dept., METU _____

Assoc. Prof. Dr. Şimşek Demir
Electrical and Electronics Engineering Dept., METU _____

Assoc. Prof. Dr. Sencer Koç
Electrical and Electronics Engineering Dept., METU _____

Dr. Orhan Şengül
Chief Researcher TÜBİTAK UZAY _____

Date: 11.12.2009

I hereby declare that all information in this document has been obtained and presented in accordance with academic rules and ethical conduct. I also declare that, as required by these rules and conduct, I have fully cited and referenced all material and results that are not original to this work.

Name, Last name : Dilşad İÇÖZ

Signature :

ABSTRACT

MILIMETERWAVE FMCW RADAR DESIGN

İçöz, Dilşad
M.S., Department of Electrical and Electronics Engineering
Supervisor: Prof. Dr. Altunkan Hızal
Co-Supervisor: Assoc. Prof. Dr. Şimşek Demir

December 2009, 91 pages

In traffic radar system, Frequency Modulated Continuous Wave (FMCW) will be used since these radars are preferred in short distance and high range resolution systems.

The system to be constructed is not only a system operating with Doppler principle and detection of speed; on the contrary a functional radar is planned to be produced. In various traffic radars in use, Doppler shift constituted by the targets causing high reflection within detection field is measured and the measured speed corresponding to this shift is seen to exceed the limits. In case of cars more than one, their speeds cannot be measured separately.

In this FMCW Radar system, it is possible to identify the targets' distance and speed. The speed information of the target will be specified by Doppler frequency and also as a result of position monitoring, the speed will be determined out of the position change occurring in the unit time. These features, in multi lane road, will be used both for different lanes and also for the cars moving at the same lane but in different ranges.

The radar system designed in this study is an easy to use, low power consuming device which can be mounted into the car.

Only the active part of the system is off the shelf products and the other RF cards are designed and produced. As a result, a low cost traffic radar will be produced.

Keywords: FMCW, traffic radar.

ÖZ

MILIMETRE DALGA FMCW RADAR TASARIMI

İçöz , Dilşad
Yüksek Lisans, Elektrik-Elektronik Mühendisliği Bölümü
Tez Yöneticisi: Prof. Dr. Altunkan Hızal
Ortak Tez Yöneticisi: Doç. Dr. Şimşek Demir

Aralık 2009, 91 sayfa

Trafik radarı sisteminde FMCW (Frequency Modulated Continuous Wave - Frekans modüleli sürekli dalga) kullanılacaktır. FMCW radarlar kısa mesafeli ve mesafe çözünürlüğü yüksek sistemlerde tercih edilmektedir.

Yapılması düşünülen sistem sadece hız tespitine yönelik Doppler prensibi ile çalışan bir sistem değildir; aksine fonksiyonel bir radar gerçekleştirilecektir. Kullanılmakta olan çeşitli trafik radarlarında, algılama alanı içerisindeki yüksek yansıma yaratan hedeflerin (araçların) oluşturduğu Doppler kayması ölçülmekte ve bu kaymanın karşılık geldiği hızın limitleri aştığı tespit edilmektedir. Birden fazla aracın bulunması durumunda ayrı ayrı hızları tespit edilememektedir.

Bu FMCW radar sisteminde, hedeflerin mesafe (pozisyon) ve hız olarak belirlenmesi mümkün olacaktır. Hedefin hız bilgisi hem Doppler frekansından oluşturulacak hem de pozisyon izleme özelliği sayesinde birim zamanda gerçekleşen pozisyon değişikliğinden belirlenebilecektir. Bu özellikler

sayesinde, çok şeritli bir yolda, hem farklı şeritlerde hem de aynı şeritin farklı mesafelerinde yer alan araçlar ayrı ayrı tespit edilip izlenebilecektir.

Sistemin sadece aktif elemanları dışarıdan temin edilecek, anten ve RF entegrasyon kartları tasarlanıp üretilecektir

Sonuç olarak, araç içerisine yerleştirilen, düşük güç tüketimli, kullanılması kolay bir radar sistemi üretilmiş olacaktır.

Anahtar kelimeler: FMCW, Trafik Radarı

To My Family,

ACKNOWLEDGEMENTS

I would like to give my special thanks to Prof. Dr. Altunkan HIZAL for his knowledge and patience which has been invaluable during my studies.

I wish to express my thanks to Assoc. Prof. Dr. Şimşek DEMİR for sharing his experience and suggesting useful materials in my studies.

I am also grateful to Dr. Orhan ŞENGÜL for his guidance, invaluable willingness to help and encourage me in completing my thesis.

I also want to give my thanks to my colleagues Dr. Özlem ŞEN, Hacer SUNAY and Tunahan KIRILMAZ not only for their great effort while solving my problems and sharing their experiences but also for their friendly attitude in times of difficulties, I have learned a lot from them.

My special thanks also must go to Başak Gonca ÖZDEMİR for her sincere and friendly attitude and I would like to thank for her friendship, moral support at all times

I would like to thank my colleagues in Space Technologies Research Institute for such friendly research environments they had provided

I would like to also count in The Scientific and Technological Research Council of Turkey (TUBITAK) for their funds during my graduate study.

Finally, I would like to thank my Mom and Dad for their love, support and patience over the years

TABLE OF CONTENTS

LIST OF TABLES

TABLES

LIST OF FIGURES

FIGURES

CHAPTER 1

INTRODUCTION

Radars are electromagnetic systems which transmit signals to outer space and receive the echo signal coming from targets. After some implementation on the received echo signal certain features of the targets can be obtained. For instance range information can be derived from the time that echo signal has taken from transmitting to receiving or velocity of the target can be obtained by transmitting modulated signals and processing the frequency shifted echo signal. Also by using directive antennas angular location of the targets can be found by using the arriving angle of the received signal.

Radar signal is generated by a powerful transmitter and received by a sensitive receiver. Radar systems are mostly classified by the types of waveforms they use or by the operating frequency. Table1 gives radar classification based on the operating frequency.

Table 1: Radar Classification According To Frequency

Band designation	Nominal frequency range
HF	3-30 MHz
VHF	30-300 MHz
UHF	300-1000 MHz
L	1000-2000 MHz
S	2000-4000 MHz
C	4000-8000 MHz
X	8000-12000 MHz
K_u	12.0-18 GHz
K	18-27 GHz
K_a	27-40 GHz
Mm	40-300 GHz

Radars can use either pulsed signals or continuous wave signals. Considering the waveforms, in pulsed radars after transmitting a short impulse signal a break is given, so that echo signal can be received before sending a new pulse out.

By the help of the time difference between the transmitted and received signal the range of the target can easily be found. Besides, continuous wave radar systems transmit a continuous wave and by the nature of this type Doppler frequency shift can be measured.

$$f_d = \frac{2v_c}{\lambda} = \frac{2v_c f_0}{c} \tag{1.1}$$

Where;

V_c : Target's radial velocity with respect to radar

λ : wavelength

c : speed of light

f_0 : transmitter carrier frequency

If the target is moving with respect to radar, the received echo signal will be frequency shifted from the transmitted signal frequency by an amount of, $\pm f_d$, Doppler frequency. The positive sign indicates an approaching target, as the negative sign indicates a diverging target.

An unmodulated CW radar is incapable of measuring range unlike a pulse radar which is based on the time delay of the signals. However by applying a frequency modulation a timing mark can be obtained creating a reference to calculate target range. Hence, without reception break, measurement result is continuously available. [1]

1.1 FMCW Radar

Frequency modulated continuous radar is a technique to measure range as well as velocity by frequency modulation a continuous wave.

Since this technique has been used in early applications such as radio altimeters and proximity fuse, now it has a wide application area in civil industry [2].

If we have to point the advantages of this technique:

1) It has the both target's relative speed and range.
2) Modulation is easily consistent with a wide variety of solid state components whose peak power is usually a little greater than average power.
3) Since peak power is nearly same as the average power radar is less detectable by intercepting equipment.
4) Frequency measurement can be performed digitally using a processor based on the fast Fourier transform to get the range measurement.
5) It has to ability to measure small ranges to the target with minimal measured range comparable to the transmitted wavelength.
6) It has the ability to measure small range changes which is less than fractions of a percent of the wavelength.

7) Small error of range measurement, also with the same processing methods it is within hundredths of a percent.
8) After mixing the signal frequency range is from hundreds of hertz up to hundreds of kilohertz (this simplifies all microwave preselection and filtering), it is easier to handle the received waveform, as minimum bandwidth is required in the IF circuitry.
9) Another advantage is the small weight compactness and small energy consumption due to absence of high circuit voltages.

1.2 Some Applications of the FMCW Radar

1.2.1 Radar Proximity Fuzes

To detonate an explosive device automatically, a proximity fuze also called a VT fuze was designed. It works when the distance to target becomes smaller then a predetermined value or when the target passes through a given plane.
The fuze is considered one of the most important technological innovations of World War II. [16]

1.2.2 Radar Altimeters

Radar altimeters simply measure the altitude above terrain which is used under an aircraft or spacecraft in 1924, radio altimeter was invented by an American engineer.
These are also used in commercial aircraft for landing and approach in low visibility conditions and automatic landings.

1.2.3 Level Measuring

FMCW Radar technique can be used measuring the level of liquid in a tank by the help of a narrow beam width antenna pointing vertically toward the surface.

1.2.4 Navigational Radar

As FMCW radar is most useful for short ranges, it can be used for surveillance of the sea or large river port when vessels arrive under conditions of bad visibility. They can also find area of usage in measuring range and relative speed of any target within the port or for navigation radars with ranges up to several kilometers.

1.2.5 Measurement of Very Small Motions

An example for this application can be given as the observation of the vibrations of some components in machines and mechanism.
The necessity of a contactless device is provided by FMCW radar in this manner.

1.2.6 Vehicle Collision Warning Radar

Vehicle collision warning systems are developed to meet the necessities in response to substantial traffic growth in cities and on motorways. Design of the systems is difficult. Basically there are four radars located in front, tail and two sides. They are used for parking, backing and measurement of range and relative velocity for targets ahead of the vehicle.

1.2.7 Precision Range Meter for Fixed Targets

Multi frequency CW radars using phase processing of the reflected signals are used for precision range measurement. But an active reflector must be installed to simulate a Doppler shift to measure the range of fixed targets, since it is not always possible and FMCW radar is free from this disadvantage, it can be applied to such applications easily.

1.3 Basic theory of FMCW Radar

Unlike pulse radar, CW radar has no time separation between transmitted and reflected signals. Hence range information of a target is possible only if we modulate transmission signal in amplitude, phase or frequency. Since in amplitude modulation, it is practically impossible to select received signal against the interfering background, frequency modulation can be used to detect time difference between transmitted and reflected signals. This operation is carried out by multiplying these signals and getting the difference signal which carriers the range information for a stationary target.
The transmitter is a single- frequency source and a sample of the transmitted signal is fed to mixer. From a moving target a Doppler shifted return signal is produced.

This thesis is mainly about manufacturing an FMCW traffic radar for which active elements will be off the shelf products and RF integration cards will be designed and built up. Basic outline of the chapters in this study is as follows:

In Chapter 1, radar systems are defined and classified; afterwards FMCW radars are briefly explained in terms of its advantages and application areas.
In Chapter 2, FMCW radars' operating principles are studied in detail and beat frequency of moving and stationary targets are formulated.

In Chapter 3, specifications and system parameters of traffic radar are defined, minimum and maximum of beat frequencies are determined. Limitations on maximum range are evaluated. Circuit diagram is formed and the selected elements are briefly explained. The calculations on RF power consumption and noise in the receiver are performed. Finally, the effect of target's Doppler on range accuracy is examined.

In Chapter 4, the theoretical background of Branchline Coupler, its basic operation and even-odd mode analysis are described in detail. 7 dB coupler utilized in traffic radar is designed in ADS, simulated in ADS® and HFSS® programs. Also measurement results of 7 dB branchline coupler are given.

In Chapter 5, advantages, design consideration, simulation and measurement results of aperture coupled microstrip patch antenna and high pass-low pass filters are presented. The patch antenna is designed and simulated in Ensemble® and HFSS®; low pass and high pass filters are designed and simulated in FilPRO®.

In Chapter 6, a general discussion of the studied works and future works are handled.

CHAPTER 2

FMCW RADAR

This chapter obviously describes the operation principle of the FMCW Radar.

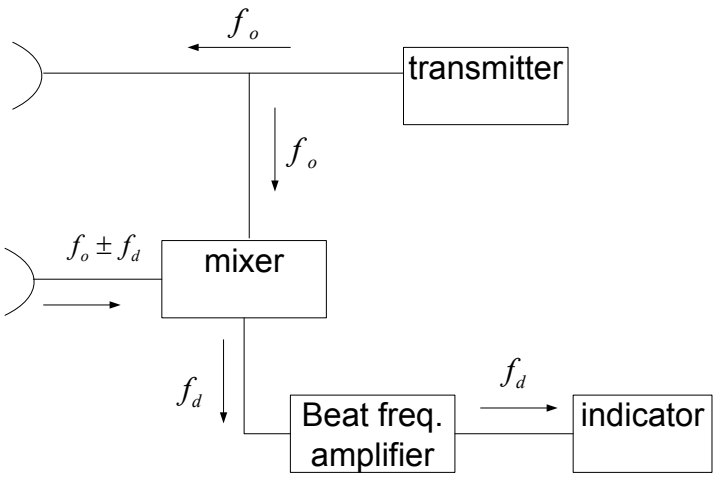

Figure 1 Simple Continuous Wave Radar Block Diagram

2.1 Frequency Modulated Continuous Wave Radar Basics

In Frequency Modulated Continuous Wave Radar a sinusoidal, linear sawtooth or triangular waveform signal can be transmitted. For a sawtooth waveform, frequency increases with time linearly.

Upon being reflected from a stationary target, a time delayed signal with the same linear frequency change can be observed. This time delay is related to the target distance, R, from transmitter [7].

$$T = \frac{2R}{C} \tag{2.1}$$

Where C is the speed of light.

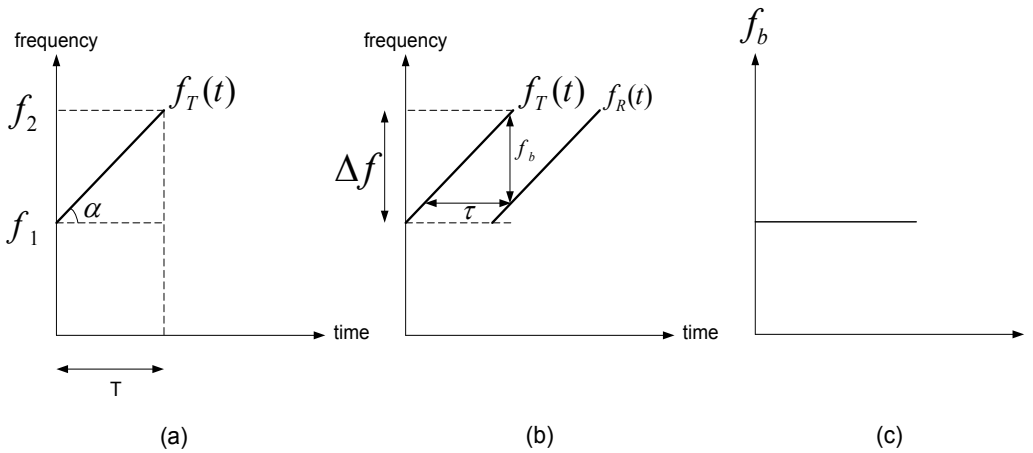

Figure 2 Transmitted Signal (a) Transmitted and Received Signals (b) Beat Frequency(c).

Reflected signal is collected by the receiver antenna and fed to a mixer with the sample of the transmitted signal. Sum of the frequencies which is much higher is filtered out, on the other hand difference signal called beat frequency or IF frequency is obtained.

Beat frequency is constant except for the turnaround regions. When target is not moving which means there is no Doppler shift, beat frequency is only due to target's range.

$f_r = f_b$

where f_r is due to target's range

In Figure 2 we can see that;

$f_{T=}f_1$ at t=0

$f_{T=}f_2$ at t=T

So, the transmitted waveform has a time varying frequency of

$$f_T(t) = f_1 + \frac{df_T}{dt} \cdot t \qquad (2.2)$$

The waveform in Figure 2 has a linearly increasing frequency sweep. Where T is called sweep period;

f_2-f_1 is the frequency deviation, Δf

Range of change in transmitted frequency is $\frac{df_T}{dt}$

Also the phase of the waveform is;

$$\phi(t) = 2\pi \int f_T(t) dt \qquad (2.3)$$

$$\phi(t) = 2\pi \int \left(f_1 + \frac{df_T}{dt} \cdot t \right) dt$$

$$\phi(t) = 2\pi \left(f_1 \, t + \frac{df_T}{dt} \cdot \frac{t^2}{2} \right)$$

assuming ϕ=0 at t=0

Since the echo signal arrives after a time delay of τ and we assume a stationary target, which means the change of frequency in time is same in return signal, we can write received signal as:

$$f_R(t) = f_1 + \frac{df_T}{dt}(t - \tau) \qquad (2.4)$$

As we know beat frequency is the difference of transmitted and received signal obtained from mixer output.

$$f_b = f_T - f_R \qquad (2.5)$$

$$f_b = f_1 + \frac{df_T}{dt} \cdot t - \left(f_1 + \frac{df_T}{dt} \cdot t - \frac{df_r}{dt} \cdot \tau \right)$$

$$f_b = \frac{df_T}{dt} \cdot \tau$$

Since;

$$\frac{df_T}{dt} = \frac{\Delta f}{T} \qquad \text{and} \qquad \tau = \frac{2R}{c}$$

$$f_b = \frac{\Delta f}{T} \cdot \frac{2R}{c} \tag{2.6}$$

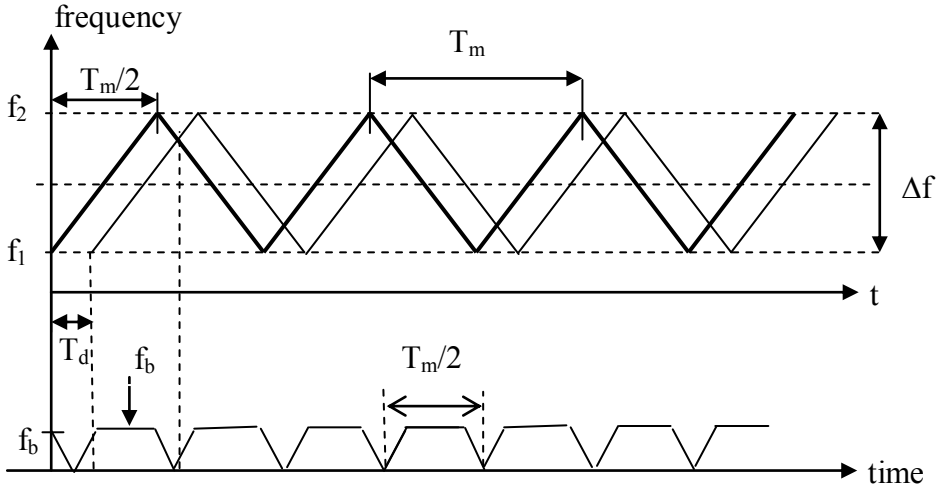

Figure 3 Triangular Frequency Modulation Waveform for Transmitted and Received Signals

Figure 3 shows a triangular frequency to implement FMCW and the resultant beat frequency. In this waveform frequency excursion Δf is limited and T_m is the modulation period.

$$f_b = \frac{\Delta f}{T_m / 2} \cdot \frac{2R}{c} \tag{2.7}$$

Or equivalently;

$$f_b = \frac{\Delta f \cdot f_m \cdot 4R}{c} \quad , \tag{2.8}$$

where f_m is the modulation frequency.

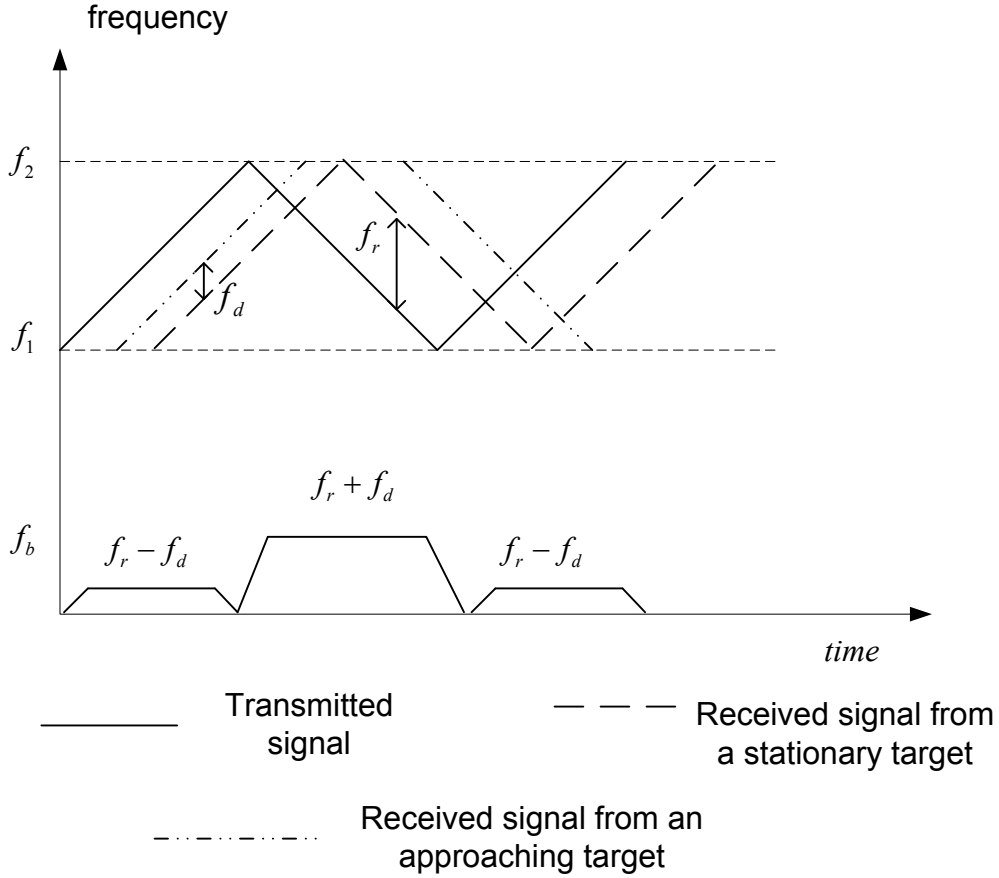

Figure 4 Transmitted and Received Signals for an Approaching Target

Now considering a moving target having a component of velocity toward or away from radar, there will be a Doppler frequency component added to or subtracted from difference frequency (beat frequency). For a closing target Doppler frequency has a plus sign and for a receding target Doppler frequency has a minus sign. [7]

If range of the target is R, then total number of wavelengths in the travel of signal from transmitter to target and return is $\frac{2R}{\lambda}$.

Since one wavelength corresponds to a phase change of 2π.

Total phase change in this time is

$$\phi = 2\pi \cdot \frac{2R}{\lambda} = \frac{4\pi R}{\lambda} \tag{2.9}$$

Since distance changes, phase is also changing and if we take derivative of this equation with respect to time, we can find the rate of change of phase which is called angular velocity [1],

$$w_d = 2\pi f_d \tag{2.10}$$

$$w_d = \frac{d\phi}{dt} = 4\pi \cdot \frac{1}{\lambda} \cdot \frac{dR}{dt}$$

Since $\frac{dR}{dt}$ change of range according to time is the radial velocity as we know.

So,

$$w_d = \frac{4\pi}{\lambda} \cdot V_r = 2\pi f_d \tag{2.11}$$

Then,

$$f_d = \frac{2 \cdot V \cdot \cos\theta \cdot f_T}{c} \tag{2.12}$$

Where;

f_T: transmitted frequency

c: speed of light

V: magnitude of the vector velocity

So, superimpose of Doppler shift on beat frequency yields uncertainty on target range [8].

This situation can be corrected by determining beat frequency over many periods of FM waveform and averaging them.

Now, $f_b = f_r \pm f_d$

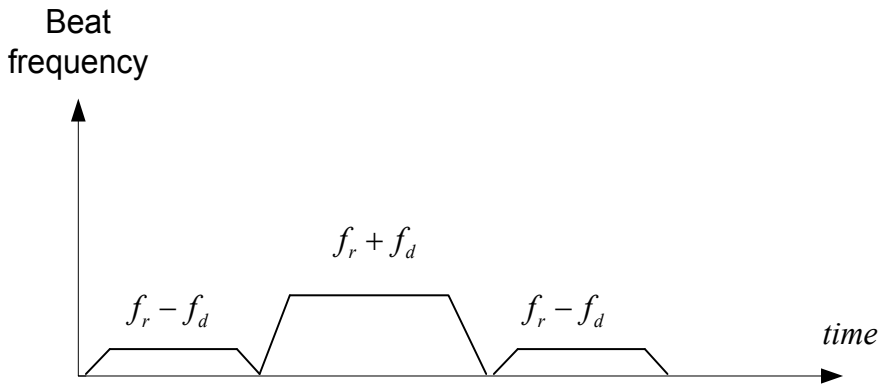

Figure 5 Beat Frequency of a Moving Object

Therefore measured difference signal is;

$f_b = f_r - f_d$ for $\frac{df_T}{dt}$ is positive

$f_b = f_r + f_d$ for $\frac{df_T}{dt}$ is negative

$$f_{b(upsweep)} = \frac{4 \cdot f_m \cdot \Delta f \cdot R}{c} - \frac{2 \cdot V_r \cdot f_T}{c} \tag{2.13}$$

$$f_{b(downsweep)} = \frac{4 \cdot f_m \cdot \Delta f \cdot R}{c} + \frac{2 \cdot V_r \cdot f_T}{c} \tag{2.14}$$

Adding the above equations we obtain range information;

$$R = \frac{c}{8.f_m.\Delta f} \cdot \left(f_{b(upsweep)} + f_{b(downsweep)} \right) \tag{2.15}$$

Multiple targets at a variety of ranges will produce multiple-frequency outputs from the mixer and frequently are handled in the receiver by using multiple range bin filters. [6]

Subtracting the equation, we can get the expression for velocity as;

$$V = \frac{c}{4 \cdot f_t} \cdot \left(f_{b(downsweep)} - f_{b(upsweep)} \right) \tag{2.16}$$

So, one complete ranging cycle should occur to obtain R and V information during the target illumination period.

2.2 Determining The Beat Frequency

FMCW Radars operate using the homodyne technique in which a sample of the transmitter frequency from sweep oscillator is serving as local oscillator for the mixer and mixed with the reflected signal from target [1].

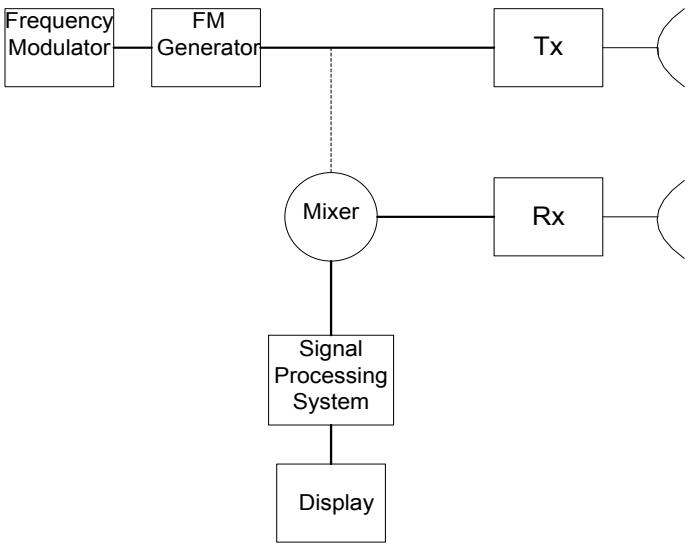

Figure 6 Basic Block Diagram of FMCW Radar with Two Antennas

Since the echo signal receives after a T_d time, beat frequency (difference of transmitted and received signal) is directly proportional to round trip time [9].

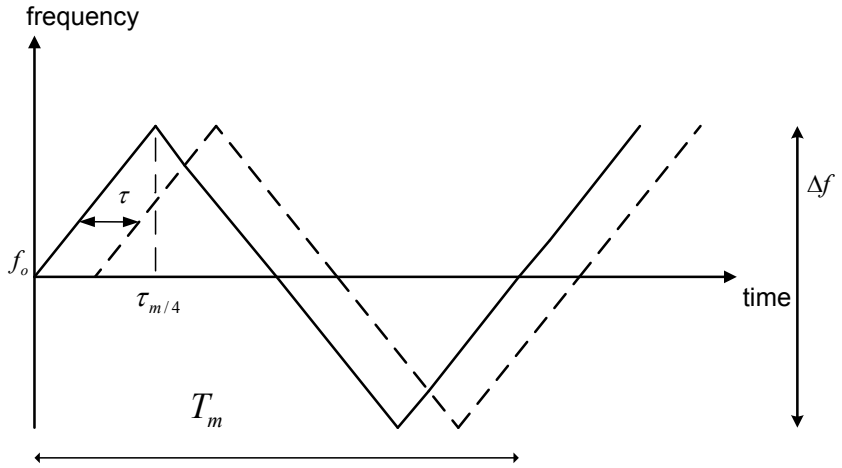

Figure 7 Transmitted and Received Signals

From Figure 7 we can describe two equations for upsweeping and down sweeping portions as;

$f^{+} = f_0 + \alpha t$ (2.17)

$f^{-} = f_0 - \alpha t$ (2.18)

where;

α: chirp rate is;

$$\alpha = \frac{\Delta f / 2}{T_m / 4} = \frac{2 \cdot \Delta f}{T_m} = 2 \cdot \Delta f \cdot f_m \quad (2.19)$$

Transmission frequency is:

$f_T(t) = f_0 + \alpha t$

where,

f_0 = transmitter frequency at time t=0

f_T =instantaneous transmitter frequency

By integrating this equation, the standing phase of the transmitted signal can be found as;

$$\phi(t) = 2\pi \int f_T(t)dt \tag{2.20}$$

$$= 2\pi\left(f_0 \cdot t + \frac{\alpha t^2}{2} \right)$$

Assuming phase is zero at t=0.

Now, the modulated transmitted frequency is;

$$V_t(t) = A_t \cdot \sin(\phi(t)) \tag{2.21}$$

If we put equation (2.20) into equation (2.21):

$$V_t(t) = A_t \cdot \sin(2\pi(f_0 \cdot t + \frac{\alpha t^2}{2})) \tag{2.22}$$

The received echo signal from target is delayed and attenuated version of the transmitted signal;

$$V_r(t-\tau) = A_r \cdot \sin(2\pi \cdot (f_0 \cdot (t-\tau) + \frac{\alpha}{2} \cdot (t-\tau)^2)) \tag{2.23}$$

The IF signal, which is the mixer output signal, is the product of these signals. Using the known trigonometric calculations, we obtain;

$$\sin a \cdot \sin b = \frac{1}{2} \cdot \left[\cos(a-b) - \cos(a+b)\right]$$

$$V_{out}(t) = \frac{1}{2} \cdot A_t \cdot A_r \cdot \left[\begin{array}{l} \cos(2\pi f_0 t + \frac{2\pi\alpha t^2}{2} - 2\pi f_0 t + 2\pi f_0 \tau - 2\pi \frac{\alpha}{2}(t-\tau)^2) - \\ \cos(2\pi f_0 t + \frac{2\pi\alpha t^2}{2} + 2\pi f_0 t - 2\pi f_0 \tau + \frac{2\pi\alpha}{2}(t-\tau)^2) \end{array} \right]$$

$$V_{out}(t) = \frac{1}{2} \cdot A_t \cdot A_r \cdot \left[\cos 2\pi(\alpha\tau t + (f_0\tau - \frac{\alpha}{2}\tau^2)) - \cos 2\pi((2f_0 - \alpha\tau)t + \alpha t^2 + (\frac{\alpha}{2}\tau^2 - \tau f_0) \right] \quad (2.24)$$

The second cosine term describes a linearly increasing signal (chirp) at about twice the carrier frequency with a phase shift proportional to round trip time, τ as in Figure 8

This term is filtered out by using low pass filter after mixer. The first cosine term describes the beat frequency (IF frequency) with a fixed frequency that is obtained by differentiating the instantaneous phase term with respect to time.

$$f_b(t) = \frac{1}{2\pi} \cdot \frac{d}{dt}(2\pi(\alpha\tau t + (f_0\tau - \frac{\alpha}{2}\tau^2))) \quad (2.25)$$

$$f_b(t) = \alpha\tau \quad (2.26)$$

Or equivalently;

$$f_b(t) = 2 \cdot \Delta f \cdot f_m \cdot \tau = 2 \cdot \Delta f \cdot f_m \cdot \frac{2R}{c} \quad (2.27)$$

$$f_b(t) = \frac{4 \cdot \Delta f \cdot f_m \cdot R}{c} \quad (2.28)$$

which is the same with the result found before.

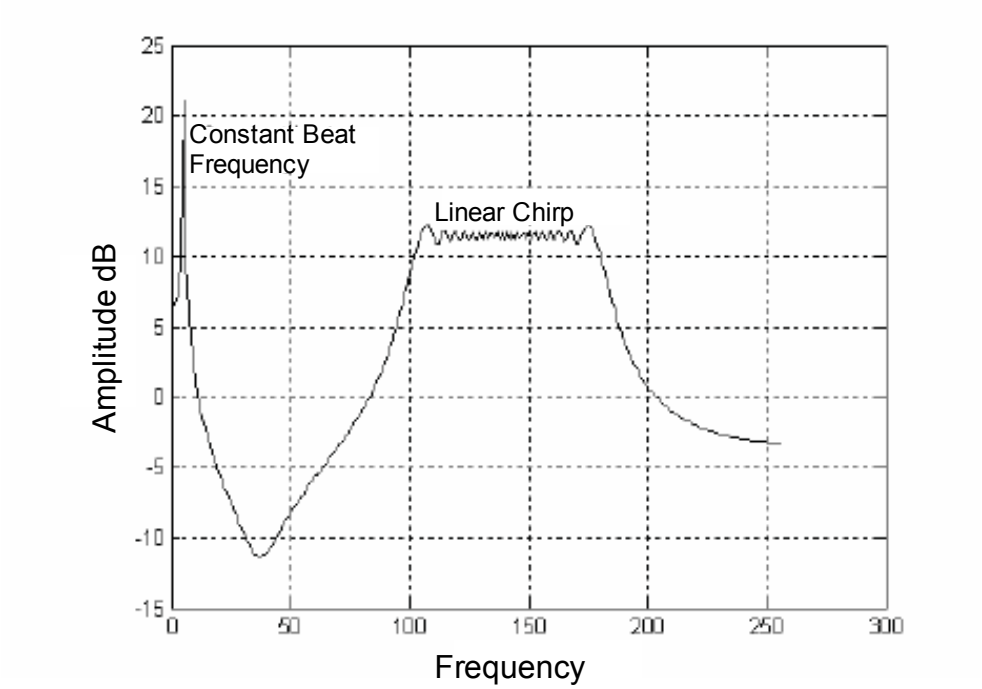

Figure 8 FMCW Radar Mixer Output Spectrum [5]

For moving targets beat frequency depends on both range and velocity.

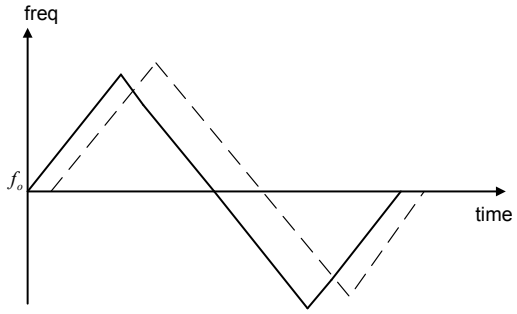

Figure 9 Transmitted Signal and Echo Signal from a Moving Target

So, we have to take into account the target's motion. If target is moving, distance becomes dependent on the velocity.

$$r(t) = r_1 + vt \tag{2.29}$$

Where r_1 : range of target at time t=0

t: time since start of sweep

v: radial velocity of the target

$\tau = \frac{2r(t)}{c}$ is the time delay

Putting the range equation in the above equation results

$\tau = \frac{2(r_1 + vt)}{c}$ Then calling the first part of the equation (2.24) and using this value of τ , we can obtain beat frequency as

$$f_b = \frac{1}{2} A_r A_t [\cos 2\pi(\alpha t . \frac{2(r_1 + vt)}{c} + f_0 . \frac{2(r_1 + vt)}{c} - \frac{\alpha}{2} . \left(\frac{2(r_1 + vt)}{c} \right)^2)] \tag{2.30}$$

After several manipulations, beat signal becomes

$$f_b = \frac{1}{2} A_r A_t \left[\cos 2\pi \left(\frac{2r_1 \alpha t}{c} (1 - \frac{2v}{c}) + \frac{2vtf_0}{c} + \frac{2\alpha v t^2}{c} (1 - \frac{v}{c}) + 2(f_0 - \frac{\alpha r_1}{c}) \frac{r_1}{c} \right) \right] \tag{2.31}$$

This expression contains time varying frequency terms and not time varying phase terms.

The first frequency term $\frac{2r_1 \alpha t}{c}(1 - \frac{2v}{c})$ is the range beat that is directly proportional to range of target. The second frequency term $\frac{2vtf_0}{c}$ is the Doppler shift which is a known result.

The third frequency term, $\frac{2\alpha v t^2}{c}(1 - \frac{v}{c})$, may be evaluated as chirp on beat range due to changing range or evaluated as chirp on Doppler shift due to changing transmitter frequency.

The fourth term $\frac{4\pi r_1}{c}(f_0 - \frac{\alpha r_1}{c})$ is the constant phase term. [5]

2.3 Radar Equation

The factors affecting the radar performance can be brought together in the radar equation that gives radar range.

In order to drive the radar equation, we can start from power density at range R from an isotropic antenna which is $\frac{P_t}{4\pi R^2}$

As we know antenna gain is

$$G_t = \frac{\text{max power density radiated by a directive antenna}}{\text{power density radiated by a lossless isotropic antenna with the same power input}}$$

Hence power density at range R from a directive antenna is $\frac{G_t P_t}{4\pi R^2}$

Radar cross section (σ), which is the effective area that scatters back the power isotropically to the receiver, determines the power density returned back to radar.

So re-radiated power density back at the radar is $\frac{G_t.P_t}{4\pi R^2}.\frac{\bar{\sigma}}{4\pi R^2}$

Where $4\pi R^2$ term below $\bar{\sigma}$ (m^2) which is the mean RCS of target; is the isotropic spreading of intercepted power.

The receiving antenna which has an effective aperture area A_{eff} intercepts this power which is as follows:

$$P_r = \frac{G_t.P_t}{4\pi R^2} \cdot \frac{\bar{\sigma}}{4\pi R^2} .A_{eff} \tag{2.32}$$

Where A_{eff} = (antenna aperture efficiency) x (actual area)

If P_r is the minimum detectable signal sum, the maximum range is obtained as;

$$R_{\max}^4 = \frac{G_t.P_t.A_{eff}\bar{\sigma}}{(4\pi)^2 S_{\min}} \tag{2.33}$$

If the same antenna is used for transmitting and receiving G_t and A_{eff} are related by:

$$G_t = 4\pi \frac{A_{eff}}{\lambda^2} \tag{2.34}$$

Where λ is the wavelength of the radar electromagnetic energy, so the minimum received signal power at the receiving antenna terminals is as follows:

$$S_{\min} = P_r = \frac{P_t \cdot G_t^2 \cdot \bar{\sigma} \cdot \lambda^2}{(4\pi)^3 \cdot R_{\max}^4} \tag{2.35}$$

This is used for rough computations because it does not include various losses.

CHAPTER 3

TRAFFIC RADAR SYSTEM

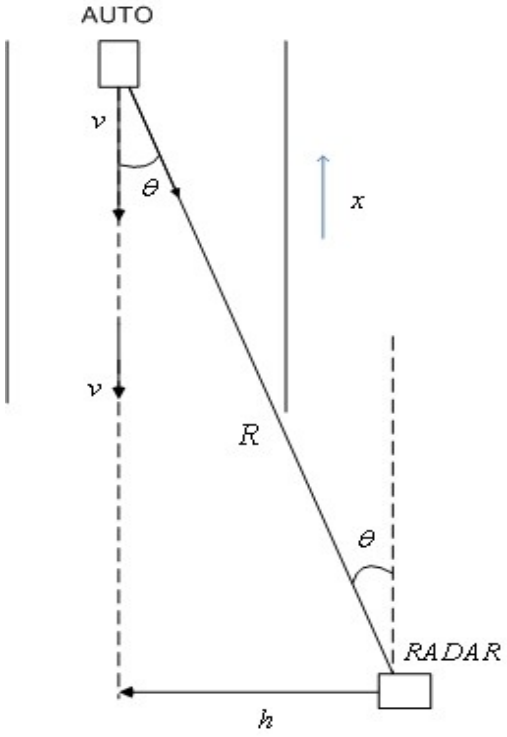

Figure 10 Block Diagram of Traffic Radar

3.1 Specifications of the RADAR

This FMCW modulated traffic radar provides range and velocity information.

- Range is between 50m-1000m
- Range resolution is 50 cm
- Doppler velocity is higher than 80 km/h

- Provides multi target tracking
- Detection time is less than 50 msec
- Maximum target displacement, Δx, is less than 2 meters at 100 km/hr
- Detection probability is higher than 0.85
- False alarm probability is less than 10-5

3.2 FMCW RADAR System Parameters

3.2.1 Frequency Band:

In order to reduce the size of the antenna structure which has a key role on the determination of the whole system size and because of the restrictions on the frequency band that is inflicted by resolution requirements, K-band is selected to be the operating frequency. Within K-band, 25.2 GHz is chosen as centre frequency for which the atmospheric attenuation is low.

3.2.2 FM Frequency deviation : Δf

Higher fm frequency deviation provides better range resolution but the most important restriction is the number of FFT points that is used in digital signal processor. [17]
Hence the FM frequency deviation is chosen 300 MHz.

3.2.3 FM modulation frequency : fm

FM frequency modulation is chosen as 500 Hz

3.2.4 The Range Resolution : ΔR

As we know that at maximum range $f_{b,max}=K.R_{max}$

Where K is Beat frequency slope $K = \frac{4.\Delta f.f_m}{c}$

The sampling rate according to Nyquist criteria is the twice of the maximum frequency component.

$f_s= 2.f_{b,max}=2.K.R_{max}$ (3.1)

The FFT will be applied to Tm/2 interval with a rate of f_s, so the FFT interval is

$T_f= Tm/2$ (3.2)

The number of samples in this time interval is $N_s = T_f / T_s$ (3.3)

Hence putting the equations (3.1) and (3.2) in the above equation gives the result as

$N_s = f_s / 2f_m$ (3.4)

Since frequency resolution of FFT , $\Delta f_b = 1/T_f$ (3.5)

$\Delta f_b = 2 /T_m =2f_m$ (3.6)

$f_b = K.R$ is also known. Then $\Delta f_b = K.\Delta R$ (3.7)

Using equations (3.6) and (3.7) one can obtain $2f_m = K.\Delta R$

Then $\Delta R = 2f_m/ K = 2f_m\, c/ 4f_m\Delta f$

$\Delta R = c / 2\Delta f$ (3.8)

Putting the values of c and Δf, range resolution is obtained as follows:

$$\Delta R = \frac{2.9979\times10^{8}}{2\times300\times10^{6}} = 0.49965 \text{ m}$$

3.2.5 Maximum Range : Rmax

From equation (3.1) we know that $f_s = 2.f_{b,max} = 2.K.R_{max}$

From equation (3.4) $f_s = N_s .2.f_m$ (3.9)

Equating these two yields $2.K.R_{max} = N_s .2.f_m$

Then

$$N_s = \frac{K.R_{max}}{f_m} = \frac{4.\Delta f.R_{max}}{c} \quad (3.10)$$

Using the range resolution equation (3.8) number of FFT samples, N_s, can also be written as:

$$N_s = \frac{2.R_{max}}{\Delta R} \quad (3.11)$$

$$N_s.T_s = N_s/ f_s = T_m/2 = T_f \quad (3.12)$$

The maximum range limitation due to beat frequency generation in an interval less than $T_m/2$ is as follows:

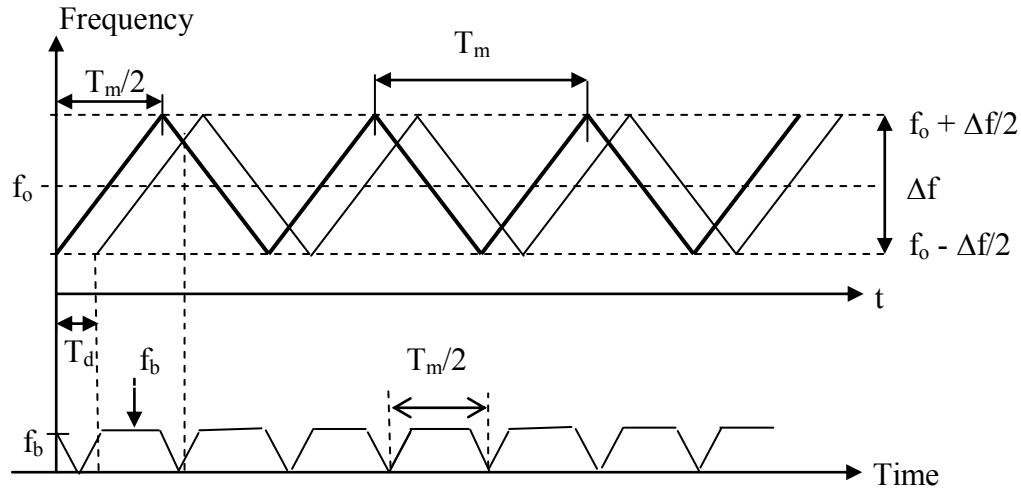

Figure 11 Transmitted and Received Signal (a) and Beat Frequency (b)

T_d is the delay time which is $\frac{2R}{C}$;

The efficiency for $T_d \leq T_m/2$ can be written as:

$$\eta = \frac{\frac{T_m}{2} - T_d}{\frac{T_m}{2}} = 1 - 2\frac{T_d}{T_m} = 1 - \frac{4 f_m R}{c};$$

$$\eta = 1 - \frac{4 f_m}{c} R \tag{3.13}$$

For $T_m/2 \leq T_d \leq T_m$ condition the transmitted and received signals are shown in Figure 12.

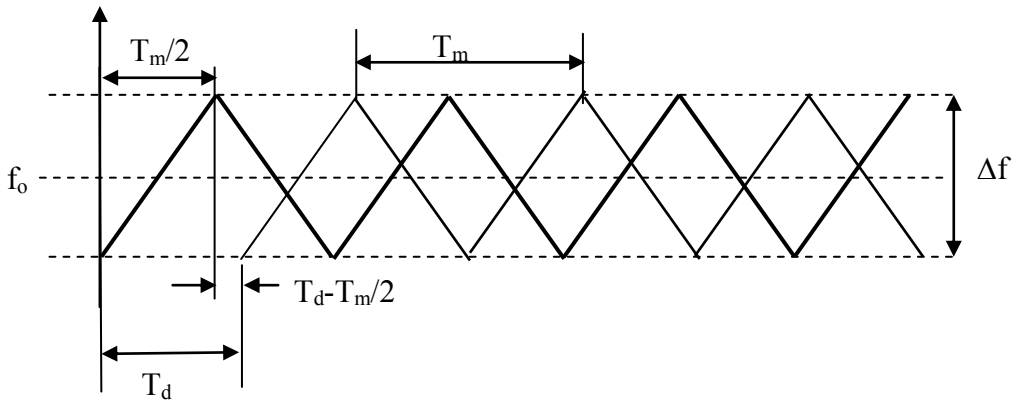

Figure 12 Transmitted and Received Signals

Slope = m= $\frac{\Delta f - f_b}{T_d - T_m/2} = \frac{\Delta f}{T_m/2}$ that yields

$$f_b = \frac{2\Delta f\left(T_m - T_d\right)}{T_m} \tag{3.14}$$

Putting the value of time delay T_d, f_b is obtained as:

$$f_b = 2\Delta f - \frac{4\Delta f . f_m}{c} R \qquad (3.15)$$

Calculation based on $f_b = \frac{4\Delta f . f_m}{c} R$ will give a range R_x by measuring f_b and calculating R_x from $R_x = f_b / K$.

The true range is related to the measured range by

$R = \frac{2\Delta f}{K} - R_x$ Which is a range ambiguity where $T_m /2 \leq T_d \leq T_m$

Besides for the condition of $T_m \leq T_d \leq 3T_m/2$, we have

$$f_b = \frac{4\Delta f . f_m}{c} R - \Delta f \qquad (3.16)$$

Hence to avoid range ambiguity, we should have

$T_d = \frac{2R}{c} < \frac{T_m}{2}$ or equivalently $R < \frac{\lambda_m}{4}$ where $\lambda_m = \frac{c}{f_m}$

For f_m =500 Hz ; λ_m =599.58 km and $\frac{\lambda_m}{4}$ = 149.8 km

So range ambiguity limitation is not critical for this design.

On the other hand the efficiency, η, limitation based on equation (3.13) can be used for the maximum range. For f_m =500 Hz

Table 2 Range vs. Efficiency

R (m)	100	1000	10000	50000
η	0.999	0.993	0.933	0.666

Hence we may limit R_{max} by limiting the η value i.e. $\eta > 0.7$

Then $\eta = 1 - \frac{4f_m}{c} R > \eta_{\min} = 0.7$

$$f_m R_{\max} < \frac{c.(1-\eta_{\min})}{4}$$

For the traffic radar design maximum range is about 1000 meters so efficiency is high enough for this range.

In this FMCW radar design for a maximum range about 1 km

$$N_s = \frac{2R_{\max}}{\Delta R} = \frac{2\times 1000}{0.49965} = 4002.8$$

So if we take $N_s = 2^{12} = 4096$ as the number of the samples

Then $R_{\max} = \frac{\Delta R.N_s}{2} = \frac{0.49965\times 2^{12}}{2} = 1023.29m$

$R_{max} < \frac{\lambda_m}{4} = 149.8$ km condition is satisfied.

$$\eta_{\min} = 1 - \frac{4f_m}{c} R_{\max} = 1 - \frac{4\times 500}{2.9979\times 10^8} 1023.29 = 0.993$$

3.2.6 Beat frequency slope, K

$$K = \frac{4f_m \Delta f}{c}$$

$$K = \frac{4\times 500\times 300\times 10^6}{2.9979\times 10^8} = 2001.40 \text{ Hz/m}$$

3.2.7 Minimum Beat Frequency : fb,min

The minimum beat frequency should be chosen as such it will be well over many f_m harmonics (M>100) so the harmonic leakage will not affect the detection of the beat signal. It is directly proportional to the minimum range, i.e.

$$f_{b,min}=K.R_{min}=M.f_m \quad (3.17)$$

Where K is the beat frequency slope, since $K=\frac{4.\Delta f.f_m}{c}$

Then $M.f_m=4.f_m.\Delta f.R_{min}/c$ (3.18)

$M=4.\Delta f.R_{min}/c$ (3.19)

is the number of harmonic

R_{min} is supposed to be 50 m, with this information M and $f_{b,min}$ values can be easily calculated.

$$f_{b,min}= K.\ R_{min} = \frac{4.\Delta f.f_m}{c}.\ R_{min} = \frac{4\times 3\times 10^8\times 500\times 50}{2.9979\times 10^8} = 100.069 \text{ kHz}$$

$M= 4.\Delta f.R_{min}/c = \frac{4\times 3\times 10^8\times 50}{2.9979\times 10^8} \simeq 200$ is the harmonic number and M> 100 condition is also satisfied.

3.2.8 Maximum beat frequency, fb, max

Maximum beat frequency corresponds to maximum range

$$f_{b,max} = K.\ R_{max} = \frac{4\times 500\times 300\times 10^6\times 1023.29}{2.9979\times 10^8} = 2048.0 \text{ kHz}$$

3.2.9 One FFT Period ,Tf :

$T_f = Tm/2 = 1/(2.500) = 1$ msec

3.2.10 Beat Frequency FFT Resolution , Δfb :

$\Delta f_b = 1/T_f = 1/10^{-3} = 1$ kHz

3.2.11 Sampling Frequency, fs :

Calling equation (3.9) minimum sampling rate can be calculated as

$f_{s,min} = N_s .2.f_m = 2^{12}.2.500 = 4096$ kHz $\cong$ 4.1 MHz

We should choose $f_s = 2.f_{s,min} = 8$ MHz.

3.2.12 Other Radar Parameters

- Power output: P_t will be 100mW=0.1W= 20 dBm
- No frequency diversity will be used
- Frequency is 25.2 GHz , $\lambda = 1.189$ cm
- Receiver Noise Figure is 3 dB
- Antenna noise temperature, $T_a = 300$ K at 25 GHz
- Antenna height is 1.5 m above ground
- Antenna gain is 9.7 dB
- Target Radar Cross Section, RCS is minimum $10m^2$ and maximum $500m^2$
- RCS= $\sigma_s = 10\ m^2$ will be used in calculations for a car
- Atmospheric attenuation, αa is 0.2 dB/ km

- Rain attenuation, αr is about 1 dB/ km

3.2.13 Losses

Process Loss is taken as 5 dB which includes beam shape loss, range straddling loss and modulation loss

Beam Shape Loss: Since the radar range calculations are usually based on the assumption that received signal strength from a target is positioned on the axis of the antenna beam, but antenna gain falls off with an angular distance from beam center. Hence a loss factor must be introduced to compensate loss in received energy due to beam shape. Beam shape loss is taken about 1.6 dB [18].

Range Straddling Loss: This loss results from reception of the signals which are not centered in a range gate or on a sampling strobe. It is defined as the required signal energy increase to achieve a given detection probability for a signal centered at a random point relative to a signal centered over the gate [7]. Range straddling loss is taken as 2 dB

Modulation loss is taken as about 1.4 dB
Transmit line loss, L_t is taken 1.5 dB
Receive line loss, L is taken 1 dB

3.3 Calculation of Signal

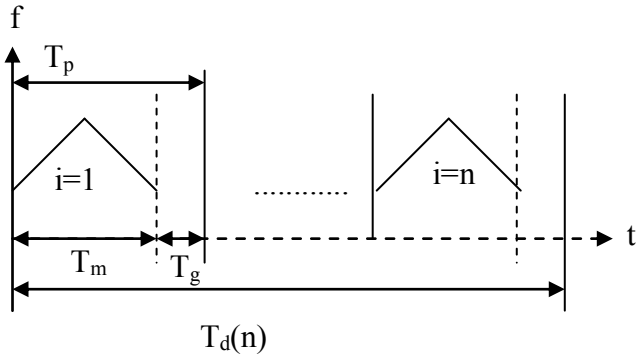

Figure 13 Transmitted Signal

n = the number of detection segments each of duration T_m =20

T_m = Detection segment = $1/f_m$ = 1/500 = 2 msec

T_g = Time gap for processing = 500 μs

T_p = T_m + T_g = 2.5 msec

$T_d(n)$ = 20 x 2.5= 50 msec

Δx = Target position displacement = 100 km/h (target velocity) x 50msec =1.4 m

3.4 Circuit Diagram

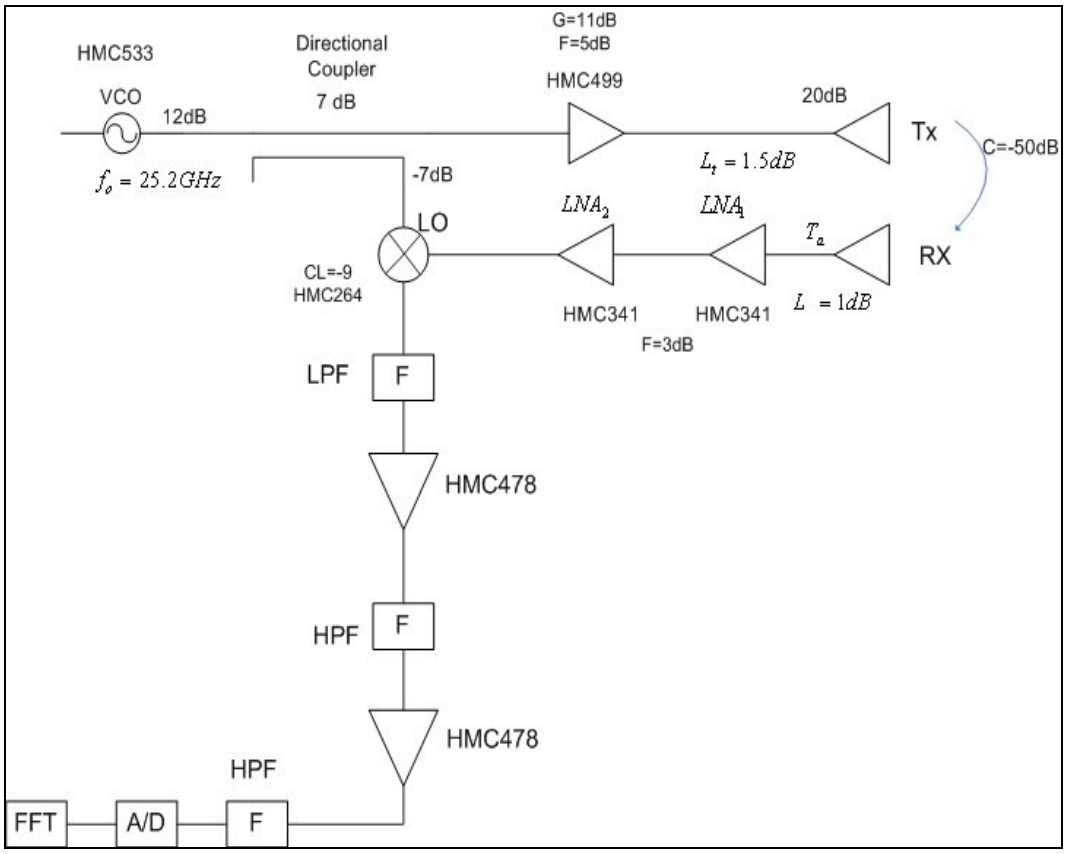

Figure 14 Circuit Diagram of the FMCW RADAR

3.4.1 Noise in The Receiver

The system noise at the antenna terminals is very important in radar system analysis because received signal level compared to noise give the target detection criteria. The receiver input noise can be calculated with the formula of:

$$N_i = k.T_s.B_n \tag{3.20}$$

Where

k : Boltzman's constant : $1.38x10^{-23} watts / Hz / K^o$

B_n : Equivalent noise bandwidth of the receiver

T_s : Equivalent system noise temperature

Equivalent system noise temperature is calculated in terms of the antenna noise temperature, receiver noise figure and transmission line losses.

The following formula is used to calculate equivalent system noise temperature:

$$T_s = T_a + (F_{recv}.L_{line} - 1).T_0 \qquad (3.21)$$

Where

T_0 : Physical temperature in K^0 of the receiver which is usually taken as 290^0K

F_{recv} : Total noise figure of the receiver

L_{line} : Radar's one way receiver line losses from antenna to the receiver input.

T_a :Antenna noise temperature which will be used as 300^0K in our calculations.

From phase noise curve of VCO noise floor is -140 dBc

Transferring the transmit noise to the receive part we obtain

+12 -140+11-50= -167 dBm

Then Tc = 1445.86 K^o Which is calculated for 1 Hz bandwidth with the formula of Ns

$$-167 = 10\log(1.38\times10^{-23}\times1\times T_c\times1000)$$

Antenna noise temperature, T_a is 300 K^o, noise figure of LNA is 3 dB (from datasheet) and receive line loss is 1 dB. By using these values one can obtain the receiver noise temperature as follows.

T_a : 300^0K

L_{line} :1 dB

F_{recv} : 3 dB

T_0 : 300°K

$T_s^{'} = 300 + (10^{0.3}.10^{0.1} - 1).290$

$T_s^{'}$ = 738.45 K°

Then equivalent system noise temperature is

T_s = 738.45 + 1445.84 = 2184.29 K°

Δf_b =1 kHz = 1000 Hz

Then again using the formula of N_s

$N = 10\log(1.38\times10^{-23}\times1000\times2184.29\times1000)$

N = -135.2 dBm is the noise floor

We should take N= -130 dBm

3.4.2 RF Power Consumption

The active elements in the circuitry consume a power of about 2.5 Watts.

VCO : +5 V_{dc} x 220 mA = 1100 mW

Power Amplifier : +5 V_{dc} x 200 mA = 1000 mW

LNA : 2 x (3V_{dc} x 35 mA) = 210 mW

Mixer : 3 V_{dc} x 25 mA = 75 mW

3.4.3 Power Density At Near Range

At R=15 cm

Flux= $\frac{dP}{ds} = \frac{P_t.G}{4\pi.R^2} = \frac{100mW.10^{0.9}}{4\pi.0,15^2} = 0.28mW/cm^2$ < 10mW/cm^2

At R=10 m

$\frac{dP}{ds} = \frac{100mW.10^{0.9}}{4\pi.10^2} = 0.632mW/m^2 = 6.32x10^{-5}mW/cm^2$ << 10mW/cm^2

While determining the RF output power, not exceeding the limits which would be hazardous to human health is important. Hence staying below the limit of 10mW/cm^2 above a distance of 15 cm from the active transmitting antenna has been taken into consideration and 100 mW RF output power is enough for this conditions.

3.4.4 Signal to Noise Ratio (SNR)

The signal to noise ratio S_i/N_i at the antenna terminals is simply expressed as

$$\frac{S_i}{N_i} = \frac{P_t \times G^2 \times \bar{\sigma} \times \lambda^2}{(4\pi)^3 \times R^4 \times k \times T_s \times B_n} \tag{3.22}$$

From noise calculations we know that $N = k.T_s.B_n = -130$ dBm

By using the rough equation for the minimum detectable signal that corresponds to maximum range and minimum radar cross section, it is obtained as

$$S_{min} = P_r = \frac{P_t \times G_t{}^2 \times \sigma \times \lambda^2}{(4\pi)^3 \times R_{max}{}^4} \tag{3.23}$$

$$S_{min} = \frac{100mW \cdot (10^{0.97})^2 \cdot 10m^2 \cdot 0.011^2}{(4\pi)^3 \cdot 1000^4} = -142dBm$$

If effect of the multipath and asphalt road is included then signal to noise ratio can be written as:

$$SNR=\frac{P_t\times G^2\times\bar{\sigma}\times\lambda^2.L_a}{(4\pi)^3\times R^4\times k\times T_s\times B_n}.|F_t|^4 \qquad (3.24)$$

Where $|F_t|$ is the path propagation factor.

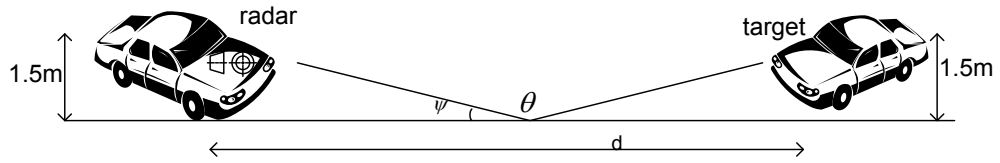

Figure 15 Radar and Target Representation

Traffic Radar is at x=0

For a distance of 500m grazing angle [21]: $\psi=\frac{h_1+h_2}{d}=\frac{3}{500}=0.34^\circ$

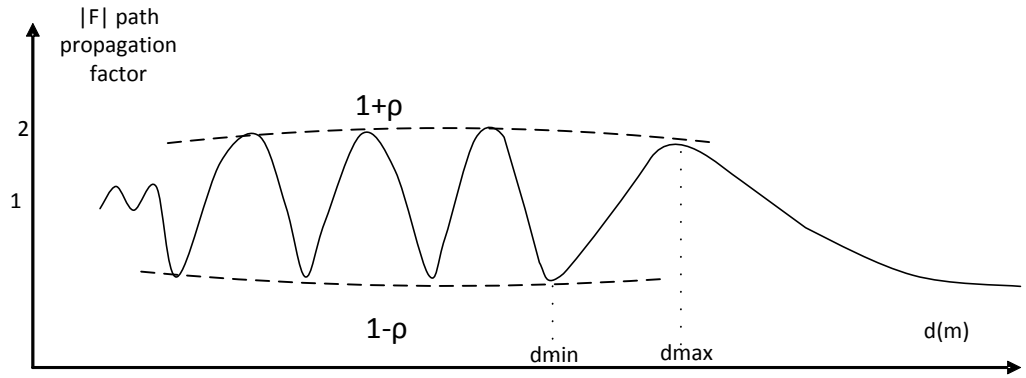

Figure 16 A Plot of |F| as Function of Distance

For practical purposes ψ is small and for most practical conditions ρ ~1 and θ~ π may be used for calculations [21]. If the formulas for maximum and minimum path propagation factor are used as:

$$d_{max,n} = \frac{4\pi h_1 h_2}{\lambda[\theta + 2(n-1)\pi]} \qquad n=1,2,3\ldots \qquad (3.25)$$

$$d_{min,n} = \frac{4\pi h_1 h_2}{\lambda[\theta + (2n-1)\pi]} \qquad n=1,2,3.. \qquad (3.26)$$

Since $h_1=h_2=1.5$m

$$d_{max} = \frac{4\pi 1.5x1.5}{0.012x\pi} = 750m \qquad \text{for n=1}$$

$$d_{min} = \frac{4\pi 1.5x1.5}{0.012x2\pi} = 375m \qquad \text{for n=1}$$

Second maximum is at 250m and minimum is at 187.5m. Thus targets (cars) are considered in the interference region. As a result between the maximum regions detection probability will drop at minimums of $|F_t|$

3.5 Traffic Radar System Theory

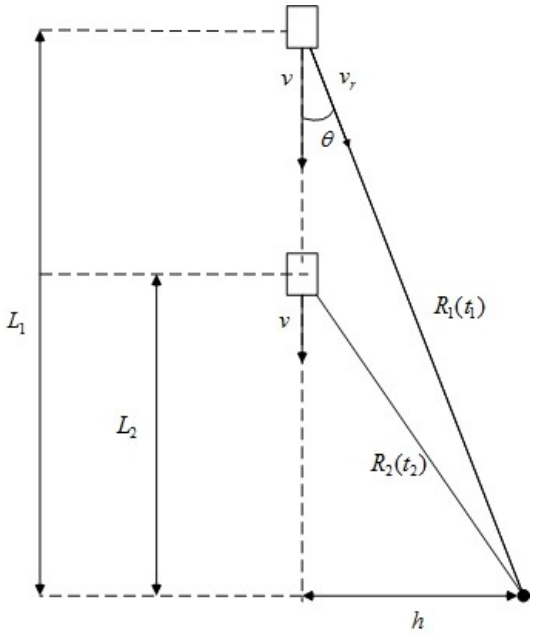

Figure 17 Radar and Target Representation

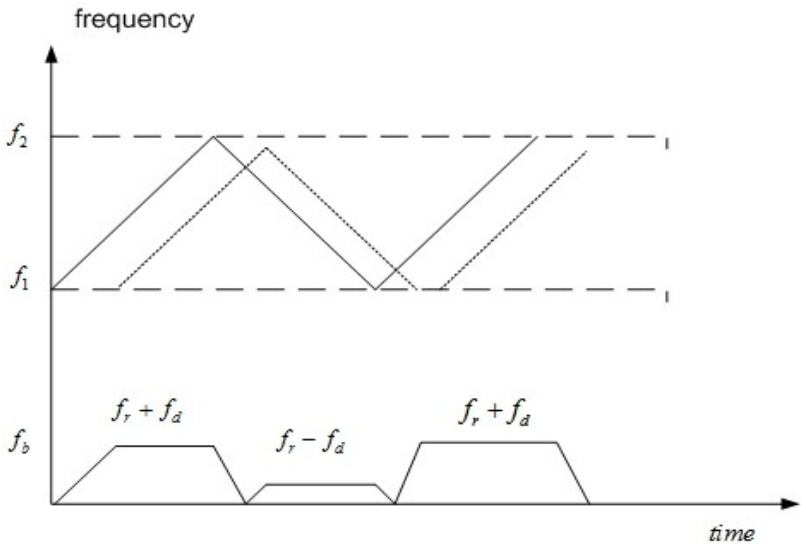

Figure 18 Transmitted and Received Signals (a), Beat Frequency (b) for Moving Target

The FMCW Radar should yield an FFT outcome in $T_m/2$ seconds. This value provides either $f_r + f_d$ or $f_r - f_d$ information. Thus to obtain the range information i.e. $f_r = K.R$ we need to average the frequency measurements such that $(f_r + f_d + f_r - f_d)/2 = f_r$ and for Doppler frequency we need $(f_r + f_d - f_r + f_d)/2 = f_d$ which may be used for the differentiation of the target Doppler from the clutter Doppler.

As we know

$$f_d = \frac{2v_r}{c} f_0 = f_d = \frac{2v\cos\theta}{c} f_0$$

Then Doppler velocity is $v = \dfrac{cf_d}{2f_0\cos\theta}$ (3.27)

Beat frequency is $f_b = K.R = \dfrac{4f_m\Delta f}{c} R$ (3.28)

From Figure 17 one can write that

$$L_1\text{-}L_2 = (R_1\text{-}R_2).\cos\theta = v.(t_2 - t_1) = \frac{cf_d}{2f_0\cos\theta}(t_2 - t_1) \quad (3.29)$$

Then $\cos\theta = \left[\dfrac{cf_d(t_2 - t_1)}{2f_0(R_1 - R_2)}\right]^{1/2}$ (3.30)

$h = R_1\sin\theta$, putting cosθ value in equation (3.29) yields

$$L_1\text{-}L_2 = (R_1\text{-}R_2).\left[\frac{cf_d(t_2 - t_1)}{2f_0(R_1 - R_2)}\right]^{1/2} \quad (3.31)$$

$$L_1\text{-}L_2 = \left[\frac{cf_d(t_2 - t_1)(R_1 - R_2)}{2f_0}\right]^{1/2} \quad (3.32)$$

Since $v = \frac{L_1 - L_2}{(t_2 - t_1)}$ then using above equation velocity can be obtained as

$$v = \left[\frac{c f_d (R_1 - R_2)}{2 f_0 (t_2 - t_1)} \right]^{1/2} \tag{3.33}$$

3.5.1 Effect of Target's Doppler on Range Accuracy

Expected Doppler frequencies are

$f_d = \frac{2v_r}{\lambda_0}$ $\lambda_0 = 0.01189m$ and 1km/h = 0.2777778 m/s

Table 3 Doppler Frequency for Different Velocity Values

For v_r = 80 km/h	f_d = 3.74 kHz
For v_r = 100 km/h	f_d = 4.672 kHz
For v_r = 120 km/h	f_d = 5.606 kHz

Beat frequency for Rmin = 50 m is $\frac{4 \times 3 \times 10^8 \times 500 \times 50}{2.9979 \times 10^8}$ = 100.069 kHz

Beat frequency for Rmax=1023.29m is $\frac{4 \times 500 \times 300 \times 10^6 \times 1023.29}{2.9979 \times 10^8} = 2048.0$ kHz

Thus the Doppler Effect on the range measurement is small. The range shift corresponding to f_d = 5.606 kHz is

$$\delta R = \frac{5606}{K} = \frac{5606}{2001.4} = 2.8 \text{ m.}$$

3.6 Active Elements

To produce the transmitter signal HMC533 LP4 evaluation board of Hittite Corporation is used. The tune voltage needs to be set to 9.2V to obtain a signal at 25.2 GHz. In order to achieve a frequency deviation of 300 MHz and modulation frequency of 500 Hz, a simple addition circuit is used to produce the tune voltage for the VCO which is shown in Figure 18. V1 is supplied from a DC source as 9.2 V, and V2 is supplied from a function generator.

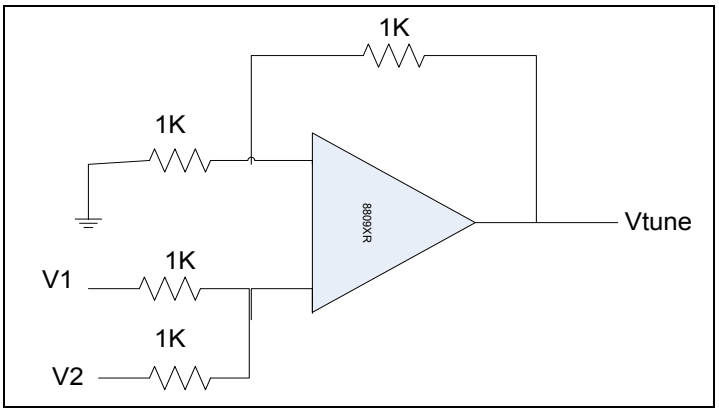

Figure 19 Addition Circuit for Tune Voltage

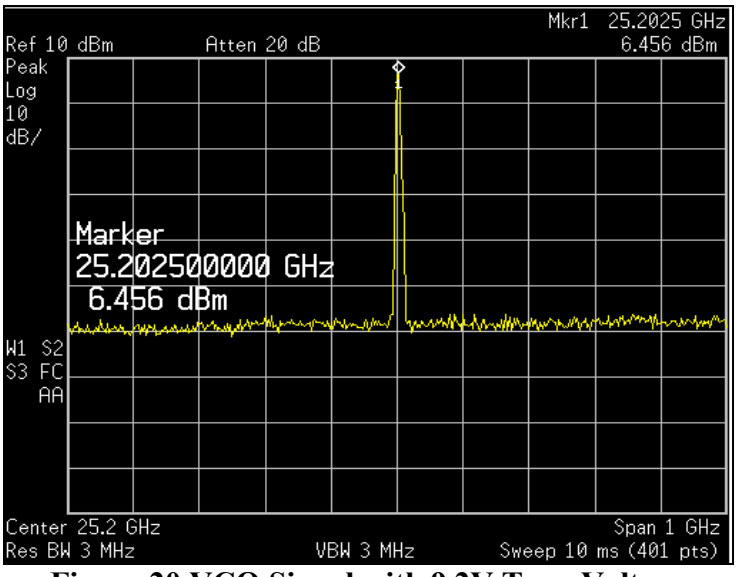

Figure 20 VCO Signal with 9.2V Tune Voltage

By decreasing the span it can be seen that VCO output is not stable since there is no loop to lock the signal, so the signal output is not a perfect triangular wave.

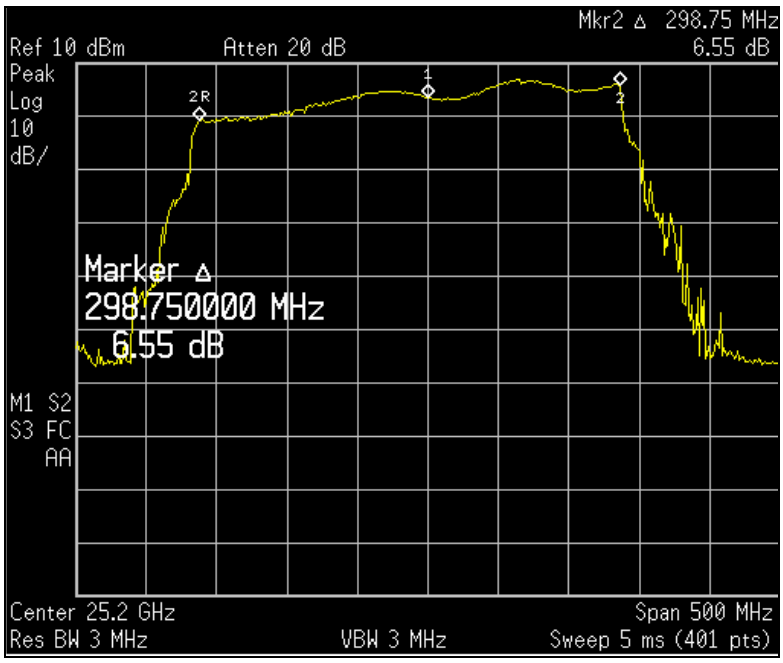

Figure 21 Transmit Signal Spectrum with Δf = 300MHz

In this measurement at least 3 dBm is needed to be added due to cable loss in this frequency. Hence output power of VCO is as expected.

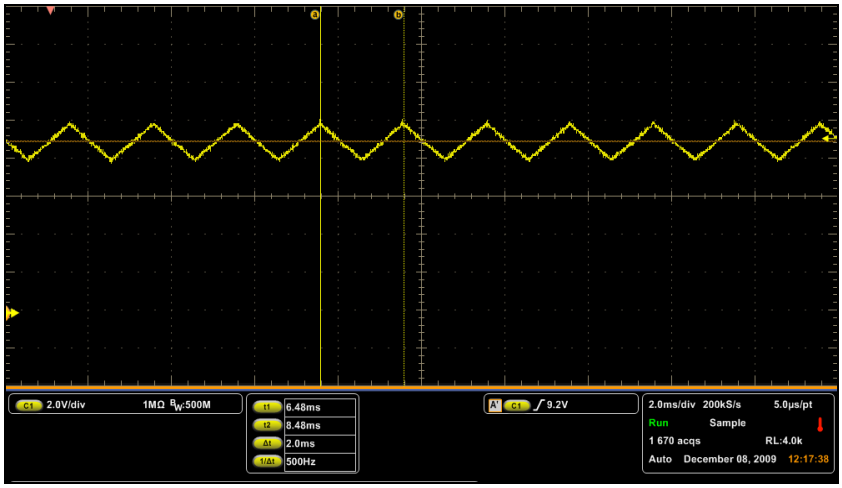

Figure 22 Tune Voltage of the VCO

CHAPTER 4

DESIGN OF BRANCHLINE COUPLER

A coupler is needed in FMCW Radar systems working with homodyne technique in order to take samples of the transmitted signal which is then mixed with the received echo signal.

In this chapter branch line coupler design parameters, simulation results and implementation results are investigated.

4.1 Theoretical Information About Branch Line Coupler

The geometry of the branch line coupler consists of two main transmission lines, which are shunt connected by two secondary lines as illustrated in Figure 23.

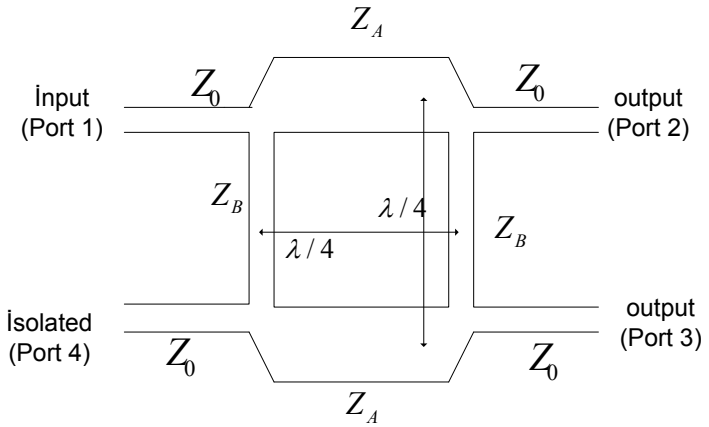

Figure 23 Branch line Coupler

4.2 Basic Operation Of The Branch Line Coupler

Basic operation of the branch line coupler is as follows; power incident at port 1 (input port) is divided between port 2 (through port) and port 3 (coupled port) equally or unequally while no power is coupled to port 4 (isolated port)

The unequal power split is achieved by varying the impedance values of the adjacent arms. Each transmission line has λ/4 wavelength that leads 90^0 phase shift between output ports [12].

In Figure 23 Z_A is the characteristic impedance of the series line and Z_B is the characteristic impedance of the shunt line. Since branch line coupler has a symmetrical structure each port can be used as input port.

Branch line couplers are usually designed in microstrip and stripline forms. In this design microstrip line is used which is shown in Figure 24.

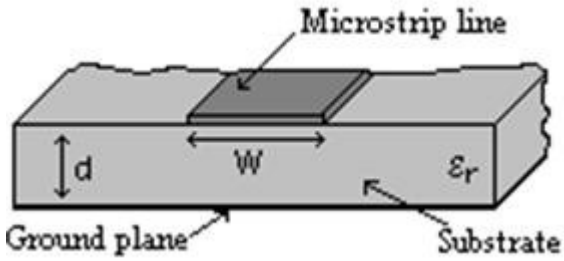

Figure 24 Geometry of Microstrip Line

4.3 Analysis Of The Branch Line Coupler

In general length of the transmission lines are chosen as quarter of the design wavelength.

Since $L = \frac{\lambda}{4}$ and $\lambda = \frac{v_p}{f}$

$$\lambda = \frac{1}{f}\frac{c}{\sqrt{\varepsilon_r}} \quad \text{and} \quad L = \frac{c}{4f\sqrt{\varepsilon_r}} \tag{4.1}$$

After choosing the Z_0 value and the substrate, W/d ratio of the microstrip line can be calculated from the formula given below [12]

$$\frac{W}{d} = \begin{cases} \dfrac{8e^A}{e^{2A}-2} \\ \dfrac{2}{\pi}\left[B - 1 - \ln(2B-1) + \dfrac{\varepsilon_r - 1}{2\varepsilon_r}\left\{ \ln(B-1) + 0.39 - \dfrac{0.61}{\varepsilon_r} \right\} \right] \end{cases} \tag{4.2}$$

First term is for $\frac{W}{d} < 2$ and second term is for $\frac{W}{d} > 2$

Where $A = \frac{Z_0}{60}\sqrt{\frac{\varepsilon_r + 1}{2}} + \frac{\varepsilon_r - 1}{\varepsilon_r + 1}\left(0.23 + \frac{0.11}{\varepsilon_r}\right)$

$$B = \frac{377\pi}{2Z_0\sqrt{\varepsilon_r}} \tag{4.3}$$

4.3.1 Even- Odd Mode Analysis

In order to find the scattering matrix of the coupler, even and odd mode analysis can be used. Assuming input voltage to port 1 is V, in even mode half of the input voltage is applied to port 1 and the other half is applied to port 4.

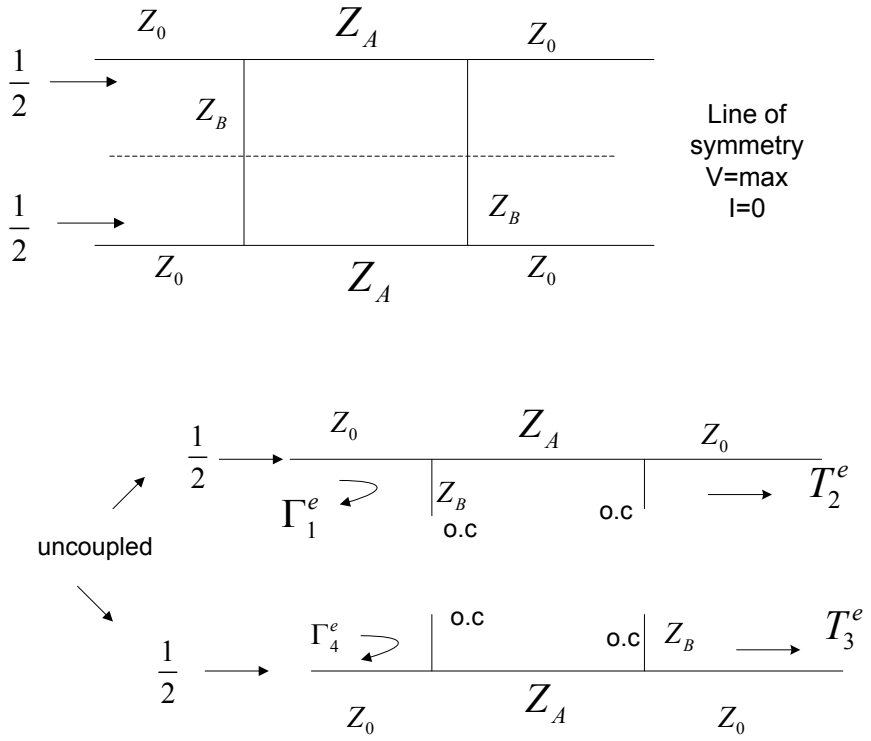

Figure 25 Even Mode Excitation

On the other hand in odd mode analysis 1/2 of the input voltage assumed to be applied at port1 while -1/2 of input voltage applied to port 4.

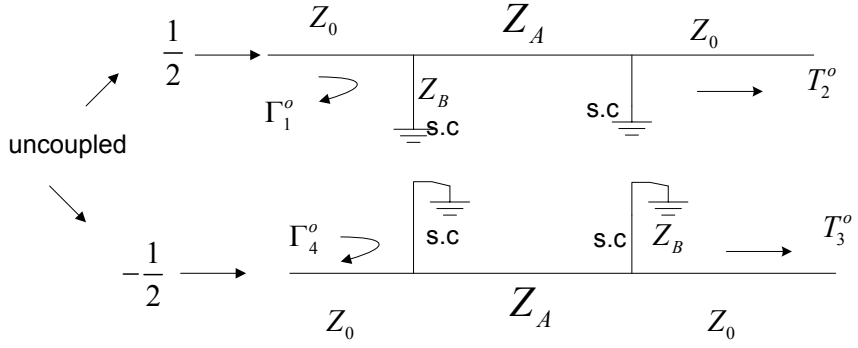

Figure 26 Odd Mode Excitation

In even mode considering the waves on the ports it is easily seen that; at port 1 there exists a reflected signal which has a reflection coefficient of Γ^e_1 and at second port there is a transmitted signal which has transmission coefficient of T^e_2.

Considering the contribution of the even mode to the ports one can obtain $\frac{V}{2}\Gamma^e_1$ at port 1, $\frac{V}{2}T^e_2$ at port 2, $\frac{V}{2}T^e_3$ at port 3 and $\frac{V}{2}\Gamma^e_4$ at port 4.

Similarly for the odd mode;

$\frac{V}{2}\Gamma^o_1$ at port1, $\frac{V}{2}T^o_2$ at port 2, $-\frac{V}{2}T^o_3$ at port 3 and $-\frac{V}{2}\Gamma^e_4$ at port 4 exist.

Now, superposition of the even and odd mode waves can be calculated at each port as following:

$$B1 = V\left[\frac{1}{2}\Gamma^e_1 + \frac{1}{2}\Gamma^o_1\right] \tag{4.4}$$

$$B2 = V\left[\frac{1}{2}T^e_2 + \frac{1}{2}T^o_2\right] \tag{4.5}$$

$$B3 = V\left[\frac{1}{2}T^e_3 - \frac{1}{2}T^o_3\right] \tag{4.6}$$

$$B4 = V\left[\frac{1}{2}\Gamma^e_4 - \frac{1}{2}\Gamma^o_4\right] \tag{4.7}$$

In order to find the overall reflection and transmission characteristics of the network, ABCD matrices will be used.

We know that $Y_A = 1/Z_A$ and $Y_B = 1/Z_B$ where Y_A and Y_B are admittances of series and shunt lines respectively.

Mainly to calculate the ABCD matrix of even mode the multiplication of each ports' ABCD matrix which consists of an open circuit stub, a series line and another open circuit stub.

$$\begin{pmatrix} A & B \\ C & D \end{pmatrix}_{even} = \begin{pmatrix} A & B \\ C & D \end{pmatrix}_{opencircuitstub} \cdot \begin{pmatrix} A & B \\ C & D \end{pmatrix}_{line} \cdot \begin{pmatrix} A & B \\ C & D \end{pmatrix}_{opencircuitstub}$$

$$= \begin{pmatrix} 1 & 0 \\ jY_B & 1 \end{pmatrix} \cdot \begin{pmatrix} \cos\beta l & jZ_A \sin\beta l \\ jY_A \sin\beta l & \cos\beta l \end{pmatrix} \cdot \begin{pmatrix} 1 & 0 \\ jY_B & 1 \end{pmatrix} \qquad (4.8)$$

Since l= λ/4 and βl = $\frac{2\pi}{\lambda} \cdot \frac{\lambda}{4} = \frac{\pi}{2}$

Then cos βl = 0 and sin βl= 1

$$\begin{pmatrix} A & B \\ C & D \end{pmatrix}_{even} = \begin{pmatrix} 1 & 0 \\ jY_B & 1 \end{pmatrix} \cdot \begin{pmatrix} 0 & jZ_A \\ jY_A & 0 \end{pmatrix} \cdot \begin{pmatrix} 1 & 0 \\ jY_B & 1 \end{pmatrix}$$

Calculating the multiplication gives even mode ABCD matrix as:

$$\begin{pmatrix} A & B \\ C & D \end{pmatrix}_{even} = \begin{pmatrix} -Y_B Z_A & jZ_A \\ j(Y_A - Y_B^2 Z_A) & -Y_B Z_A \end{pmatrix} \qquad (4.9)$$

Similarly for the odd mode, multiplication of the ABCD matrices of the short circuit stub, series line and the other short circuit stub is calculated as follows:

$$\begin{pmatrix} A & B \\ C & D \end{pmatrix}_{odd} = \begin{pmatrix} 1 & 0 \\ -jY_B & 1 \end{pmatrix} \cdot \begin{pmatrix} \cos\beta l & jZ_A \sin\beta l \\ jY_A \sin\beta l & \cos\beta l \end{pmatrix} \cdot \begin{pmatrix} 1 & 0 \\ -jY_B & 1 \end{pmatrix} \qquad (4.10)$$

Putting again cos βl = 0 ; sin βl= 1

$$\begin{pmatrix} A & B \\ C & D \end{pmatrix}_{odd} = \begin{pmatrix} 1 & 0 \\ -jY_B & 1 \end{pmatrix} \cdot \begin{pmatrix} 0 & jZ_A \\ jY_A & 0 \end{pmatrix} \cdot \begin{pmatrix} 1 & 0 \\ -jY_B & 1 \end{pmatrix}$$

Then multiplying these three matrices yields the odd mode ABCD matrix as:

$$\begin{pmatrix} A & B \\ C & D \end{pmatrix}_{odd} = \begin{pmatrix} Y_B Z_A & jZ_A \\ j(Y_A - Y_B^2 Z_A) & Y_B Z_A \end{pmatrix} \tag{4.11}$$

After this point even and odd mode reflection and transmission coefficients can be calculated from the formulas below.

$$\Gamma_1^e = \Gamma_4^e = \frac{A - D + BY_0 - CZ_0}{A + D + BY_0 + CZ_0} \tag{4.12}$$

$$\Gamma_1^o = \Gamma_4^o = \frac{A - D + BY_0 - CZ_0}{A + D + BY_0 + CZ_0} \tag{4.13}$$

$$T_2^e = T_3^e = \frac{2}{A + D + BY_0 + CZ_0} \tag{4.14}$$

$$T_2^o = T_3^o = \frac{2}{A + D + BY_0 + CZ_0} \tag{4.15}$$

Hereby, these coefficients can be calculated by putting the values of ABCD values of even and odd mode in equations 4.9 and 4.11

4.3.2 S-Parameters of the Coupler

The reflection and transmission coefficients calculated in the previous section will be used in the calculation of s-parameters of the coupler in the manner below.

$$\frac{B1}{V} = S_{11};\ \frac{B2}{V} = S_{12};\ \frac{B3}{V} = S_{13} \text{ and } \frac{B4}{V} = S_{14}$$

V is the input to port 1.

Therefore s-parameters are

$$S_{11} = \frac{1}{2}\Gamma^e + \frac{1}{2}\Gamma^o \tag{4.16}$$

$$S_{12} = \frac{1}{2}\mathrm{T}^e + \frac{1}{2}\mathrm{T}^o \tag{4.17}$$

$$S_{13} = \frac{1}{2}\mathrm{T}^e - \frac{1}{2}\mathrm{T}^o \tag{4.18}$$

$$S_{14} = \frac{1}{2}\Gamma^e - \frac{1}{2}\Gamma^o \tag{4.19}$$

4.3.3 Matching Condition

Looking at the even and odd mode ABCD parameters, in both of them equivalence of A and D parameters can be easily observed. In order to have port 4 isolated and no reflection at port 1 S11=S14=0 condition must be satisfied.
Since

$$\Gamma_e = \frac{jZ_AY_0 - jZ_0(Y_A - Y_B^2Z_A)}{-2Y_BZ_A + jZ_AY_0 + jZ_0(Y_A - Y_B^2Z_A)} \tag{4.20}$$

Then if $Z_AY_0 = Z_0(Y_A - Y_B^2Z_A)$ no power is coupled to port 4 and power input to port 1 is divided between through and coupled ports. Therefore, isolation and directivity of a matched coupler becomes very high at center frequency, in ideal case it is infinity.

4.3.4 Design Consideration

In design of unequal power split ratio branch line coupler there are three equations which contain four variables Z_1, Z_2, θ_1, θ_2 are used. One of the four variables can be chosen arbitrarily. [4]

1) $Z_1.\tan\theta_1 = - Z_2.\tan\theta_2$ (4.21)

2) $$\frac{1}{Z_1^2} - \frac{1}{Z_2^2} = \frac{1}{Z_0^2}$$ (4.22)

3) $$Z_2 \left|\sin\theta_2\right| = Z_0 \frac{k}{\sqrt{1-k^2}}$$ (4.23)

Where Z1 = characteristic impedance of series line

Z2 = characteristic impedance of shunt line

θ1 = electrical length of series line

θ2 = electrical length of shunt line

If one of the arms is chosen as $\theta_1 = 90^o$, from equation 4.21, θ_2 must also be chosen as 90^o that is the case in customary branch line coupler design.

Defining k^2 is the power division ratio as

k^2 = power out from port2/power input to port 1

Then power split ratio between through and coupled ports becomes

$$\frac{k^2}{1-k^2} = \frac{\left|S_{21}\right|^2}{\left|S_{31}\right|^2} \ .$$ (4.24)

4.3.5 Implementation of the branch line coupler

Since in this traffic radar implementation to sample transmitted signal a 7 dB coupler is required, power ratio of the input port to coupled port can be found as:

$$10\log\frac{P_1}{P_3} = 7dB \quad \text{then} \quad \frac{P_1}{P_3} = 5.011872336$$

(Power out from port2/ Power input to port 1) = $k^2 = \frac{4.011872336}{5.011872336} = 0.80473768$

No power coupling to port 4 is assumed.

θ_2 is taken as 90^0 hence using equation (4.23)

$$Z_2\left|\sin 90\right| = 50\frac{k}{\sqrt{1-k^2}}$$

Using the values of k and k^2 characteristic impedance of shunt line, Z_2 =100.15 ohm is obtained.

Calling equation (4.22), characteristic impedance of series line, Z_1 can be found as:

$$\frac{1}{Z_1^2} - \frac{1}{100.15^2} = \frac{1}{50^2}$$

Then Z_1 = 44.73 ohm

Hence these line widths are at reasonable levels for production with LPKF device.

Z_1 and Z_2 values are used as a first reference in the design of the branch line coupler in ADS2008. In order to achieve better results by varying the width and length values of the microstrip lines an optimal value is found.

In the design ROGERS RO4003C substrate is used.

RO4003C substrate thickness is h= 0.51mm

RO4003C substrate dielectric is $\varepsilon_r = 3.38 \pm 0.05$

RO4003C dissipation factor tan δ ,is = 0.0021

The branchline coupler designed for the traffic radar is simulated in ADS2008 and also HFSS simulation programs. The circuit schematics and simulation results are shown below.

The calculated lengths for the series and shunt lines are too small so the PCB dimensions become a reasonable level by inserting curve and straight 50 ohm lines at the beginning points of all ports.

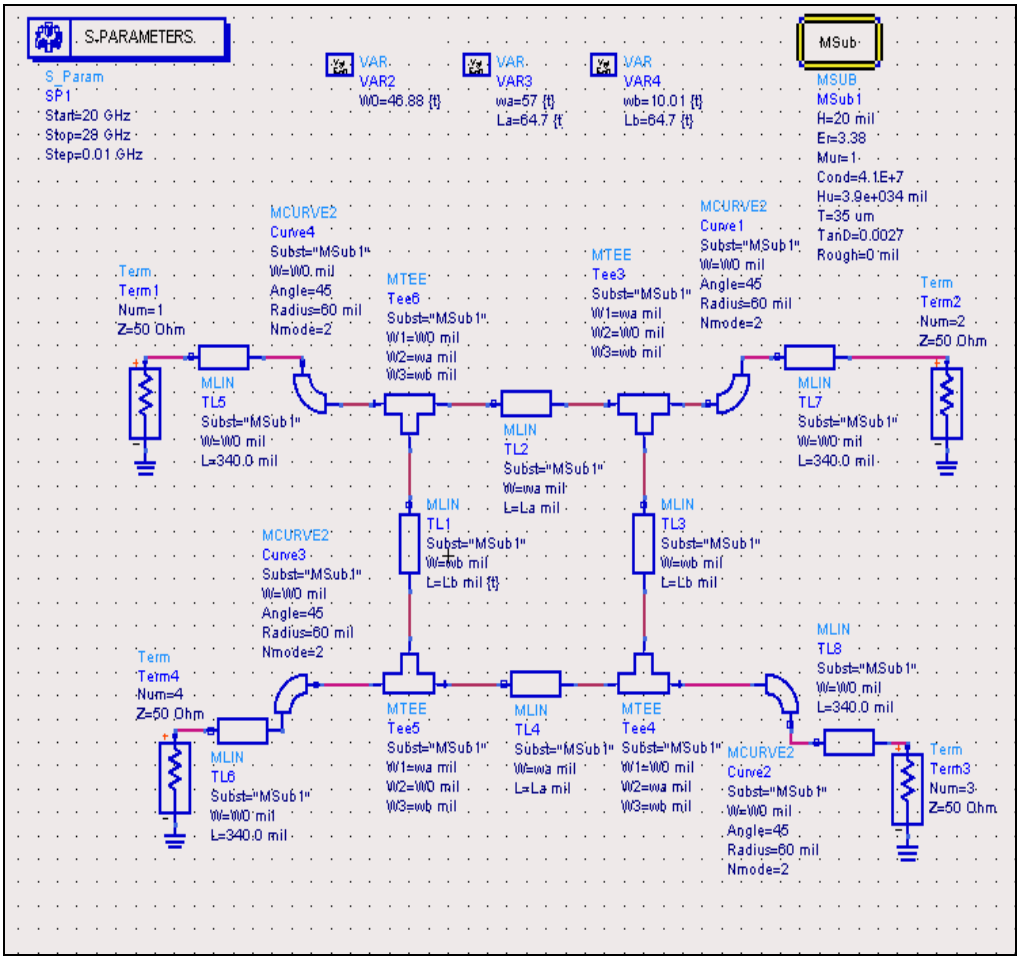

Figure 27 Circuit Schematics of 7 dB branch line Coupler in ADS

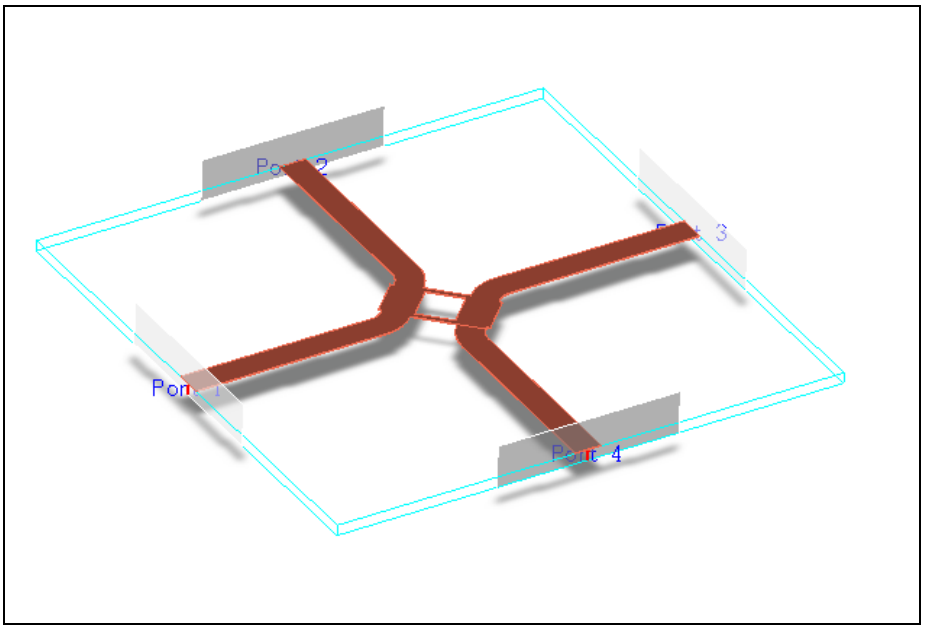

Figure 28 3D View of 7 dB Branch Line Coupler In ADS

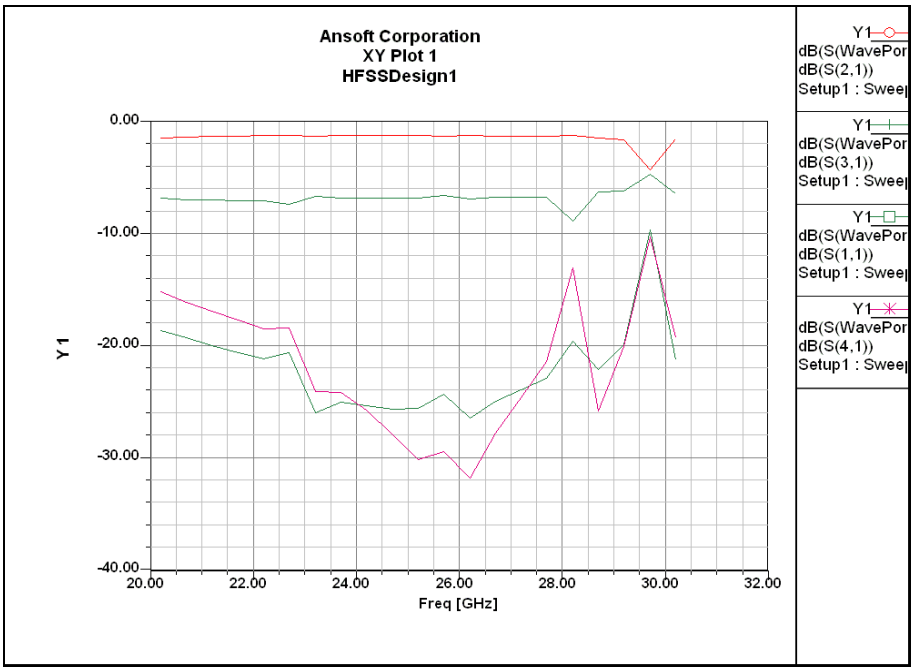

Figure 29 S-Parameters of Branch Line Coupler Simulation Results in HFSS

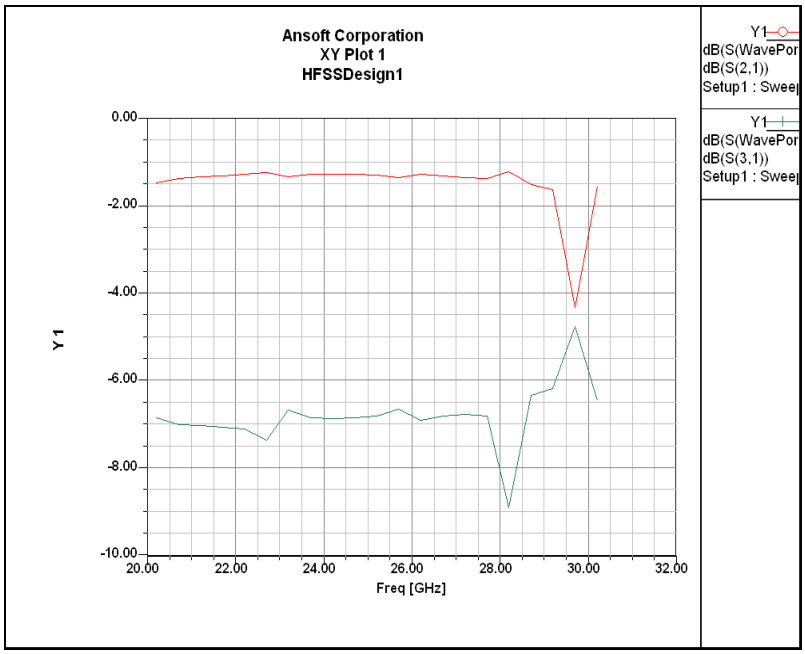

Figure 30 Simulation Results Of Through And Coupled Ports In HFSS

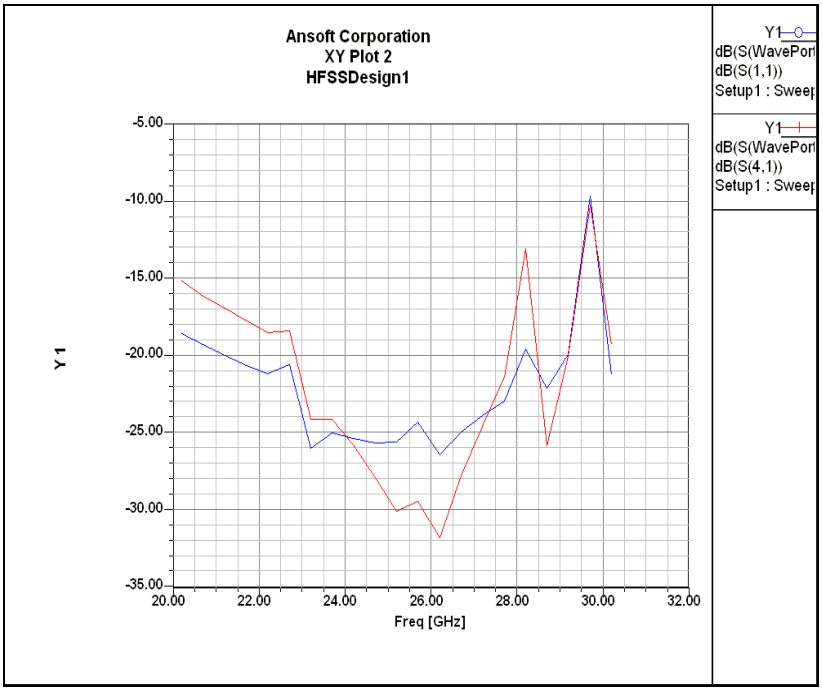

Figure 31 Simulation Results Of Input Port And Isolated Port In HFSS

4.4 Measurement Results of 7 dB Branchline Coupler

Measurement results of S parameters of the 7 dB branchline coupler which are taken from network analyzer are as follows:

Table 4 S Parameters of Branchline coupler

S parameters	Measured	Simulated
S11 (input port)	-15.9	-25
S21 (through port)	-1.59	-1.6
S31 (coupled port)	-7.6	-6.9
S41 (isolated port)	-25.8	-30

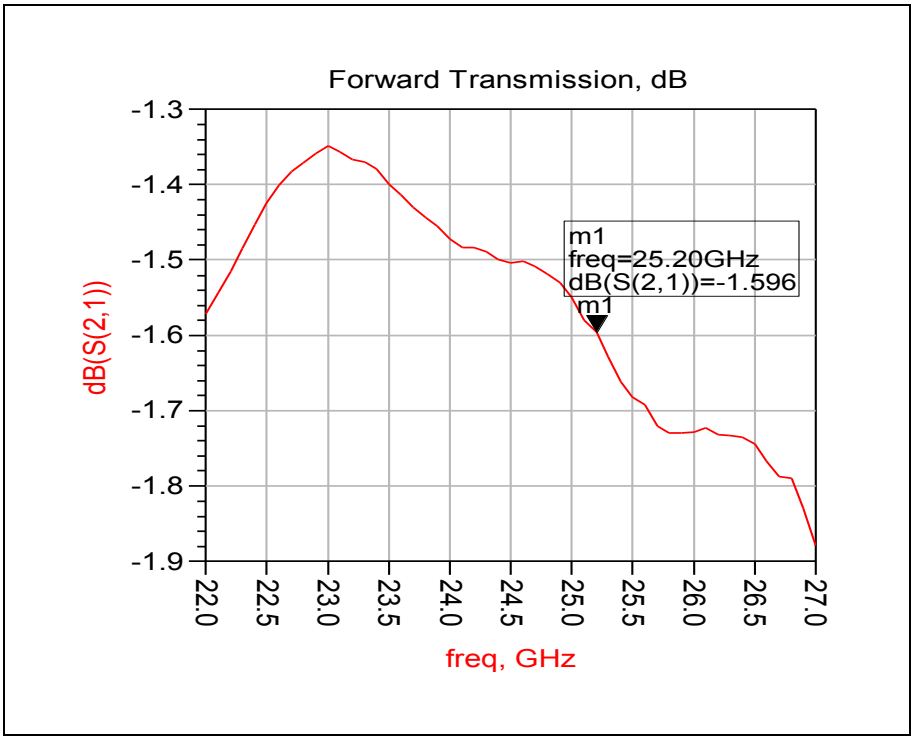

Figure 32 S_{21} Through Port Measurement Result

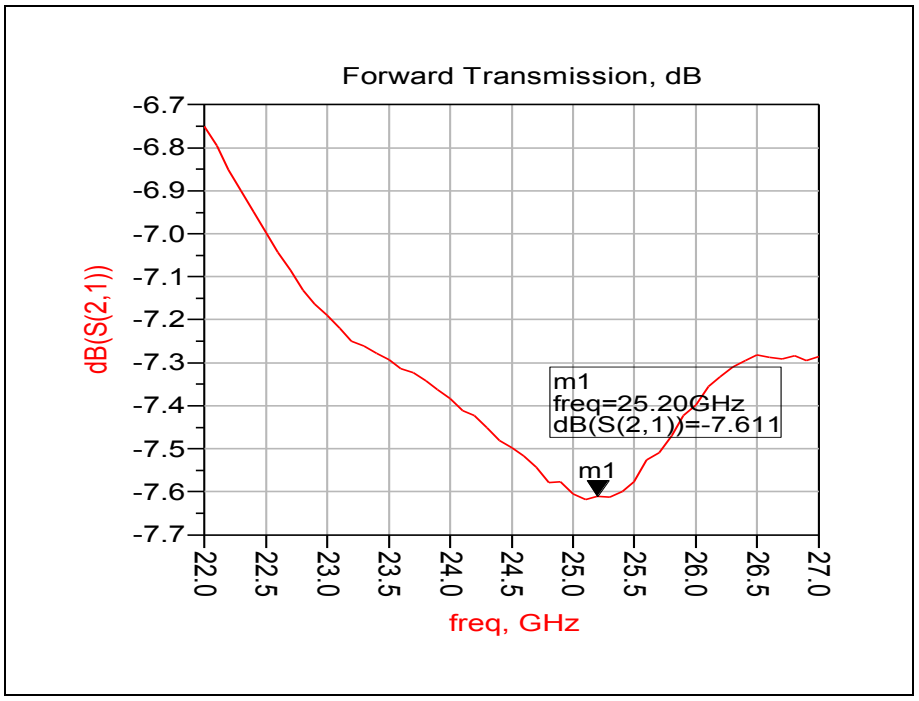

Figure 33 S_{31} Coupled Port Measurement Result

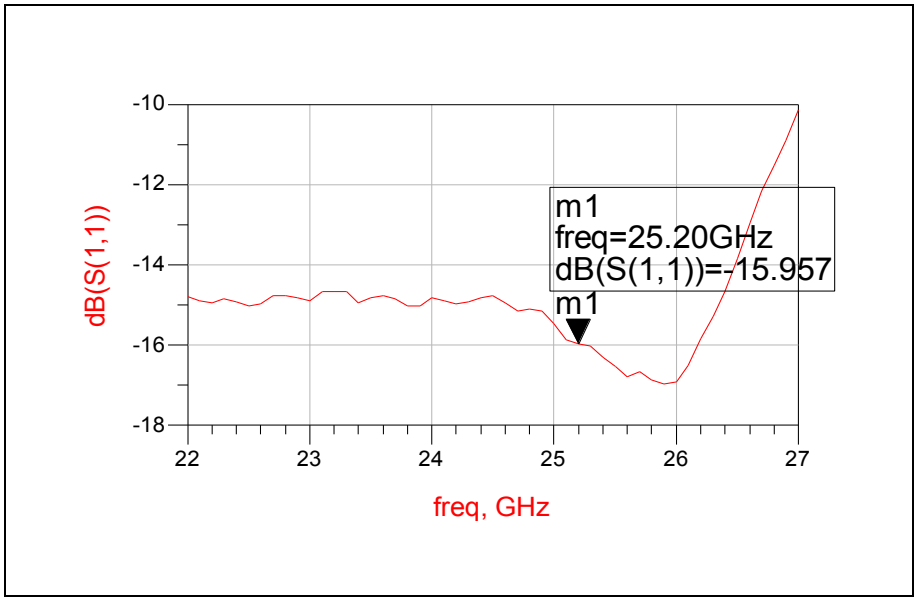

Figure 34 S_{11} Reflection of Input Port Measurement Result

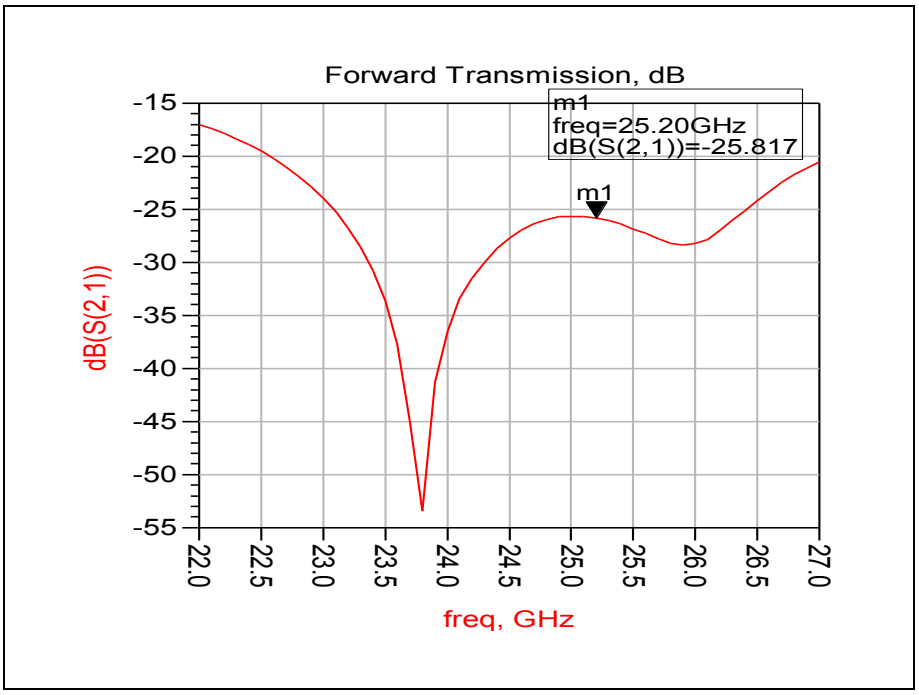

Figure 35 S_{41} Isolated Port Measurement Result

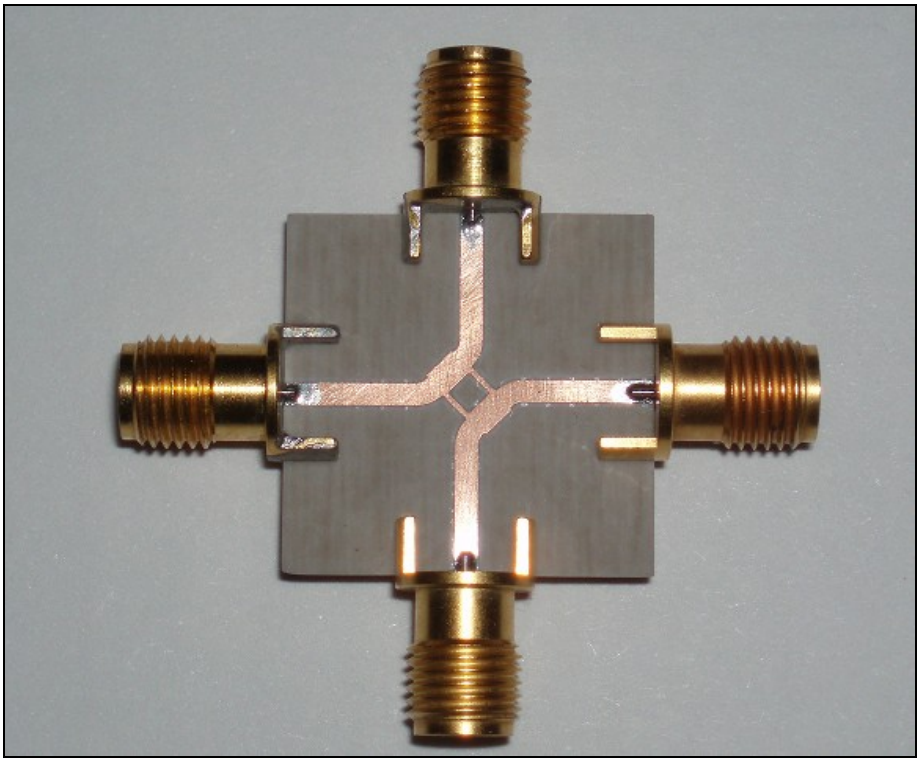

Figure 36 7 dB Branchline Coupler Circuit Implementation

S2P files which are obtained from network analyzer are drawn in ADS2008. In conclusion, through port and coupled port results are consistent with simulation results besides reflection and isolation values are acceptable in practice.

SMA connectors on 50 ohm straight line introduces loss above 10 GHz hence for proper operation using compatible connector with the frequency is important

CHAPTER 5

MICROSTRIP PATCH ANTENNAS

This chapter explains roughly the general characteristics of the microstrip patch antennas, their advantages, disadvantages and some important parameters that should be considered in the design of the microstrip patch antenna.

5.1 Introduction to Microstrip Patch Antenna

First patch antenna was fabricated in the early 1970's. They are mostly used on applications where low power, low radiation profiles are needed. The primary radiation source is the firing fields between the edges of the conductor and the ground plane behind it [15].

5.1.1 Advantages and Disadvantages of Microstrip Patch Antenna

Some of the advantages of microstrip antennas are [14]:

- Light weight, low volume and thin profile configurations
- Low fabrication cost
- Linear and circular polarizations are possible with different feed structures
- Dual frequency and dual polarization antennas can be easily made
- Cavity backing is not required
- Integration with microwave integrated circuits is easy

- Easy to manufacture, feed lines and matching networks can be fabricated simultaneously with the antenna structure

Some of the disadvantages and limitations on microstrip antennas are:

- Narrow bandwidth
- Lower gain (~ 6-9dBi)
- Large ohmic loss in the feed structure of arrays
- Most microstrip antennas radiate into half space
- Polarization purity is difficult to achieve
- For higher performance, complex feed structures are necessary
- Deduced gain and efficiency besides high levels of cross – polarization and mutual coupling in array type antennas.

The effects of parameters in aperture coupled microstrip patch antenna structure are as follows [13]:

- Antenna substrate dielectric constant affects the bandwidth and radiation efficiency. Lower permittivity gives wider impedance bandwidth and reduces surface wave excitation.
- Antenna substrate thickness affects bandwidth and coupling level with thicker substrate resulting in wider bandwidth but decreasing the coupling to aperture.
- The length of the patch radiator is important in determining the resonant frequency of the antenna.
- The resonant resistance of the antenna can be reduced with wider patch width. Square patches can be used if dual and circular polarization is required.
- Feed substrate dielectric constant is typically in the range of 2 to 10. Decreasing the thickness of the feed substrate results in less spurious radiation from feed lines, but gives higher loss.

- Slot length primarily affects the coupling level and back radiation level. Increasing the slot length provides increase in coupling to the transmission line but more than required also increases back radiation due to high power transfer.
- Slot width is another parameter affecting the coupling level but not as much as the slot length.
- Feed line width controls the characteristic impedance of the feed line in addition to affecting the coupling to slot. To a certain degree thinner transmission lines couple more to the slot.
- For maximum coupling, feed line position relative to the slot must be at right angles. Also the patch should be centered over the slot. [13]
- The length of the tuning stub is typically chosen less than $\lambda g/4$ and used to tune the excess reactance of the antenna. As the length of the stub decreases, the smith chart plot of the patch antenna impedance shifts to capacitive region.

5.2 Feeding Techniques and Structures

There are several methods of feeding the patch antenna.
Most common structures are as follows:

- Coaxial Feed
- Proximity coupled microstrip feed
- Aperture coupled microstrip feed
- Coplanar wave guide feed

For the traffic radar transmitter and receiver antennas, aperture coupled microstrip feed technique is used.

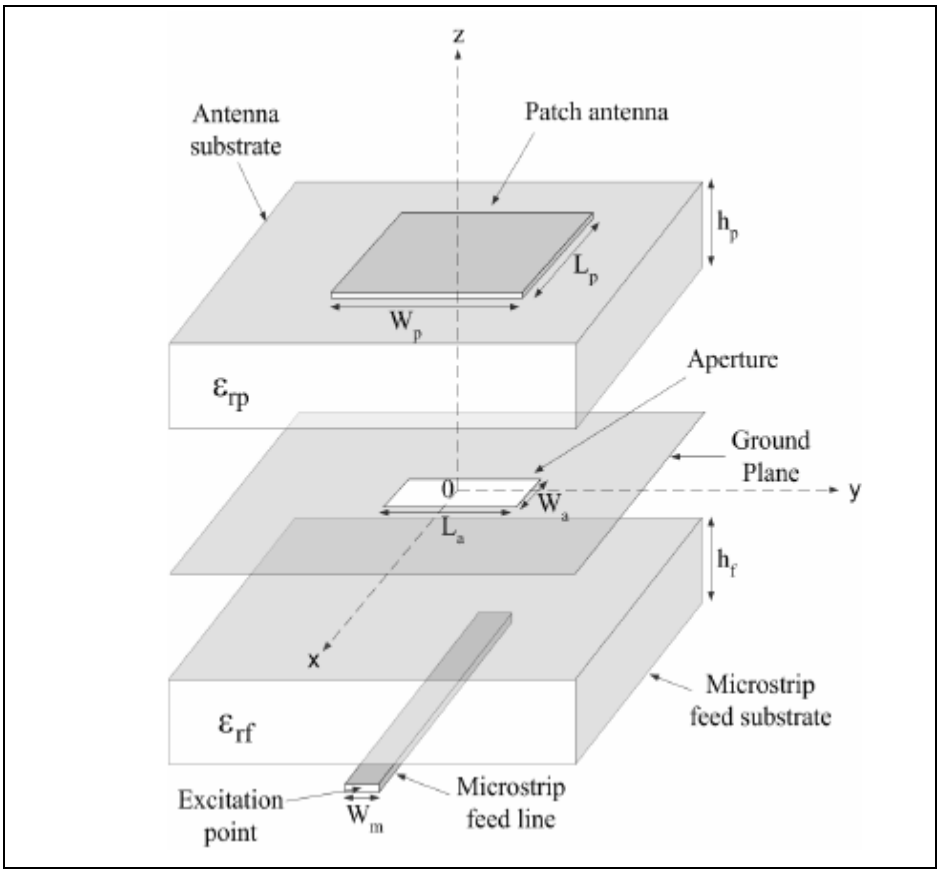

Figure 37 Expanded View of an Aperture Coupled Microstrip Patch Antenna [11]

In this technique, power comes to radiating element by coupling through a slot. The basic improvement of the structure is the ground plane which attends as an effective shield between the radiating part and the feed network. One disadvantage is that the coupling aperture radiates a small amount of power in back direction however to eliminate this radiation a ground plane located some distance below the feed layer can be used in practice.

For maximum power transfer aperture should be centered below the patch and feed line should be positioned at right angles to the center of the slot.

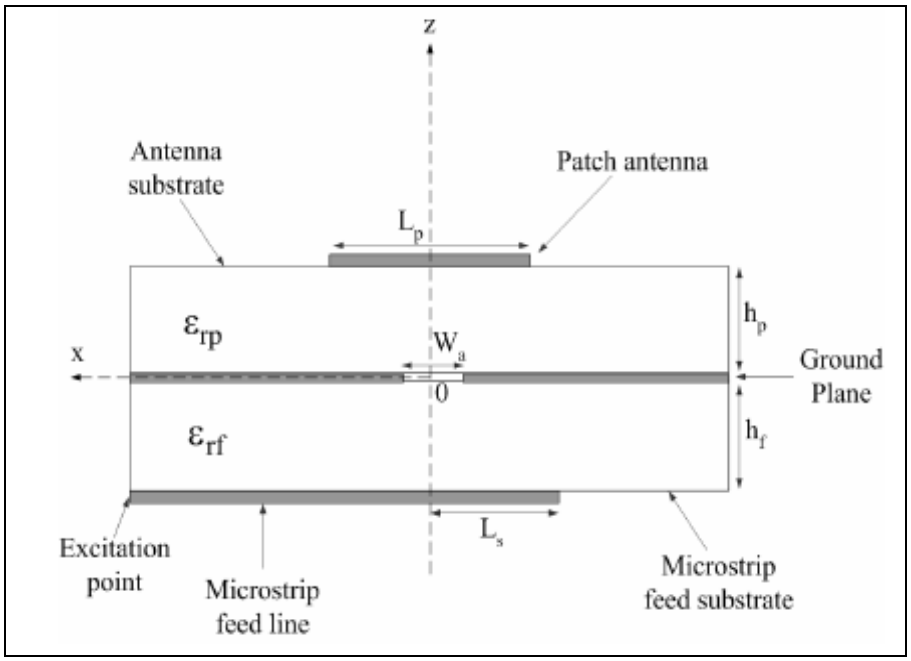

Figure 38 Side View of an Aperture Coupled Microstrip Patch Antenna [11]

Slot shape can be either circular or rectangular. In this design rectangular slot is used as these give better coupling than circular slot [19].

5.3 Aperture Coupled Microstrip Patch Antenna Design

In this design because of many advantages aperture coupled microstrip patch antenna configuration is used. To be more precise one of the advantages is using different substrate for feed line and patch. When the thickness of the substrate increases bandwidth also increases and thinner feed substrate causes the fields more confine to microstrip and decrease of back radiation. Also the choice of different dielectric constant is possible according to bandwidth and radiation efficiency requirements. Another advantage is the feeding through an aperture is easier to implement compared to a probe feed which has large self reactance.

Eventually, due to ground layer between the feed and patch antenna, spurious radiation, which can be eliminated by inserting a ground plane above, is not a problem for radiation pattern of the patch.

The design procedure started with the substrate selection. ROGERS4003C material with different heights is used for both patch and microstrip feed, considering the availability and suitability.

The design and simulation is implemented in ANSOFT ENSEMBLE. First, the layers are determined as infinite ground, trace and dielectric which are shown in Figure 39. Dielectric layers are ROGERS4003 and foam that is simulated as air between ground layer and microstrip feed.

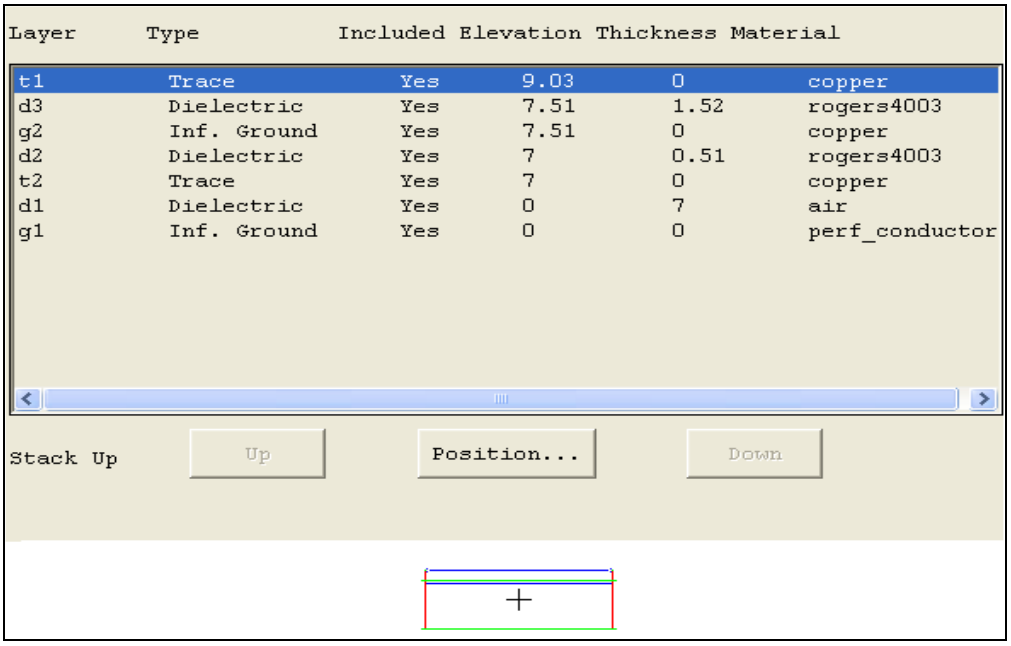

Figure 39 Patch Antenna Model definition in Ensemble

In Ensemble by using the estimate tool width of the microstrip feed line and approximate values of the patch size are determined. Then changing the slot

length, open circuit stub length and other parameters, an optimized value is obtained. The dimensions are shown in Figure 40.

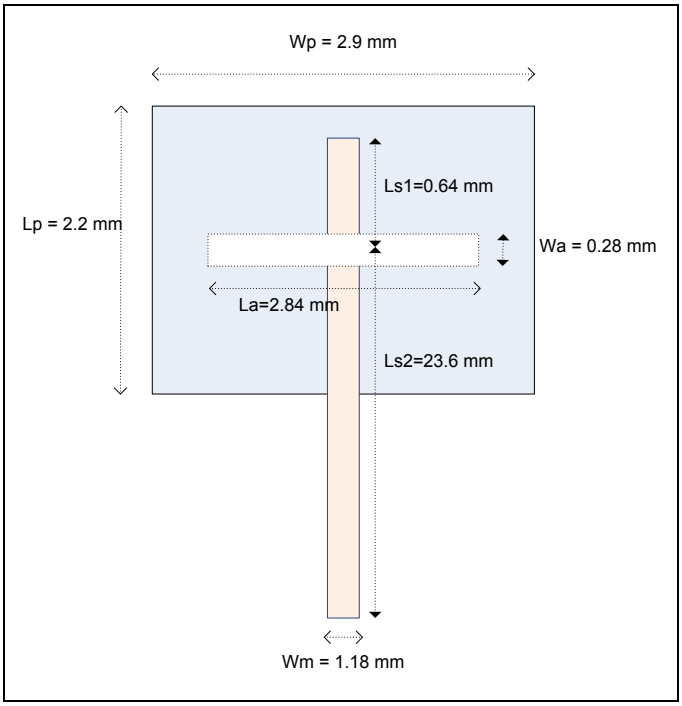

Figure 40 Aperture Coupled Microstrip Patch Antenna Design

All layers are routed on LPKF machine; the microstrip feed and the slot are on the same substrate (0.51mm) while the patch radiator is on another substrate (1.52 mm). In order to align these layers correctly four alignment points are drilled on both substrates. The aperture coupled microstrip patch antenna (ACMPA) before integration is shown in Figure 41.

Figure 41 Aperture Coupled Microstrip Patch Antenna before Integration

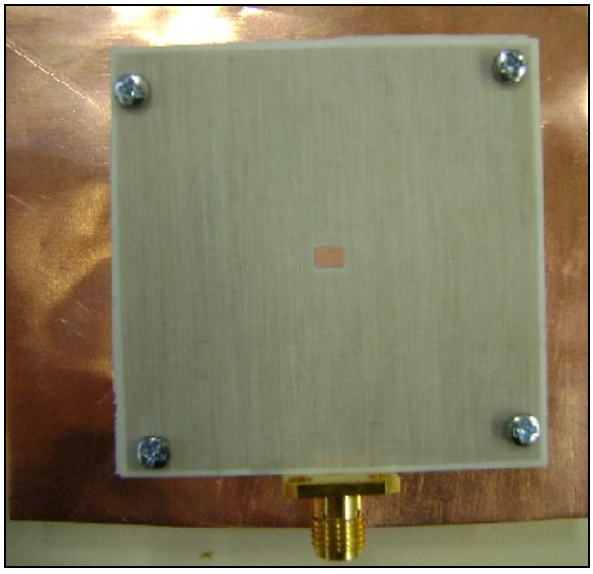

Figure 42 ACMPA after Integration

5.3.1 Simulation Results of the Antenna

Reflection at the input port of the aperture coupled microstrip patch antenna is simulated in ANSOFT ENSEMBLE which is shown in Figure 43.

The normalized E and H field radiation pattern simulations are implemented in HFSS since the effect of the finite ground plane can be taken into account in this program. The results are shown in Figure 44 and 45.

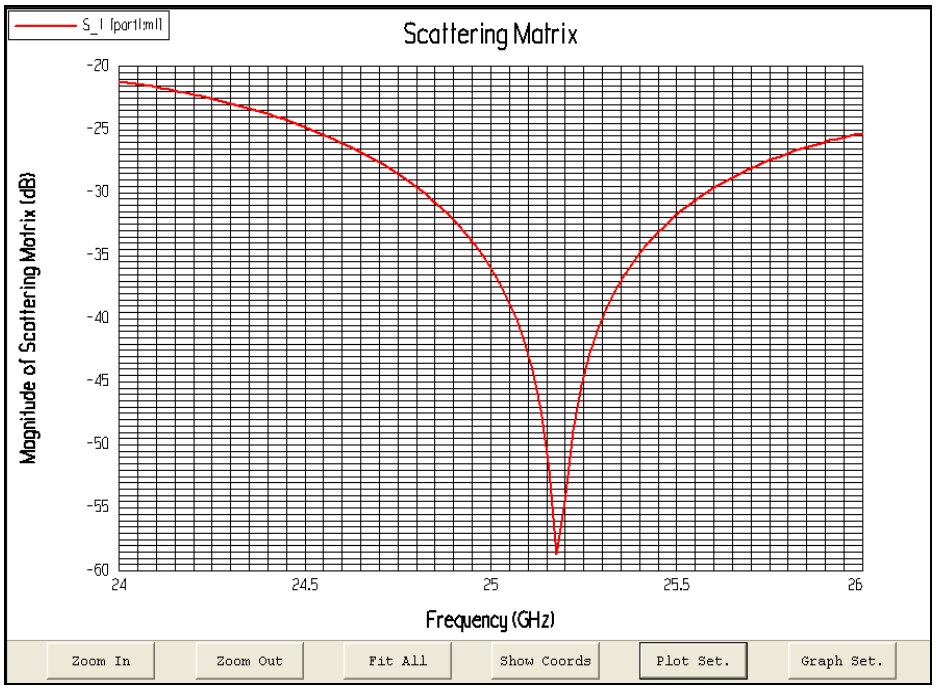

Figure 43 S_{11} Reflection factor of the antenna

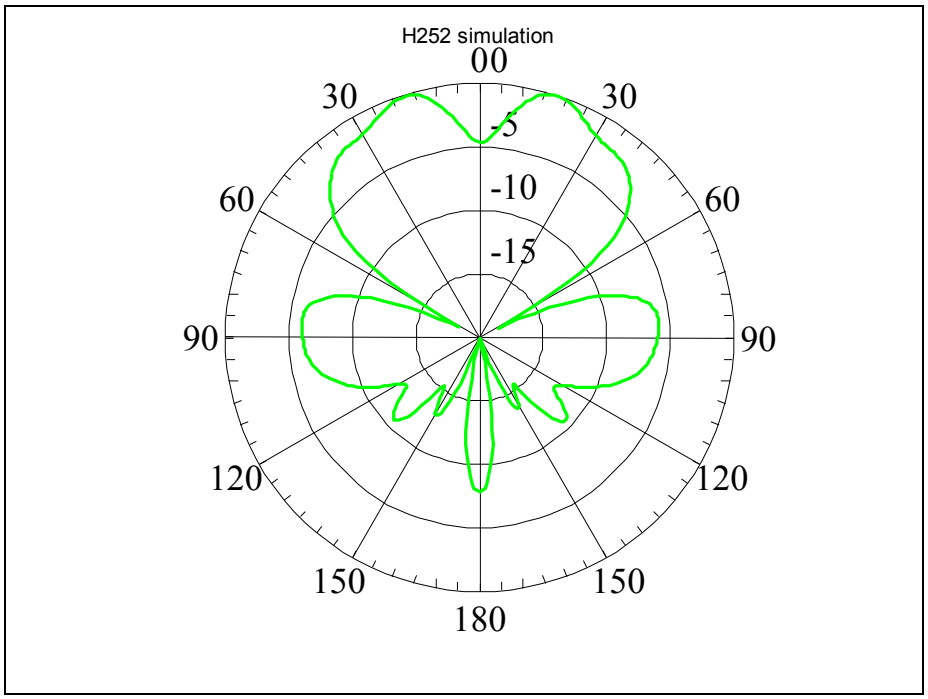

Figure 44 Simulation of Normalized H Plane Pattern at 25.2GHz

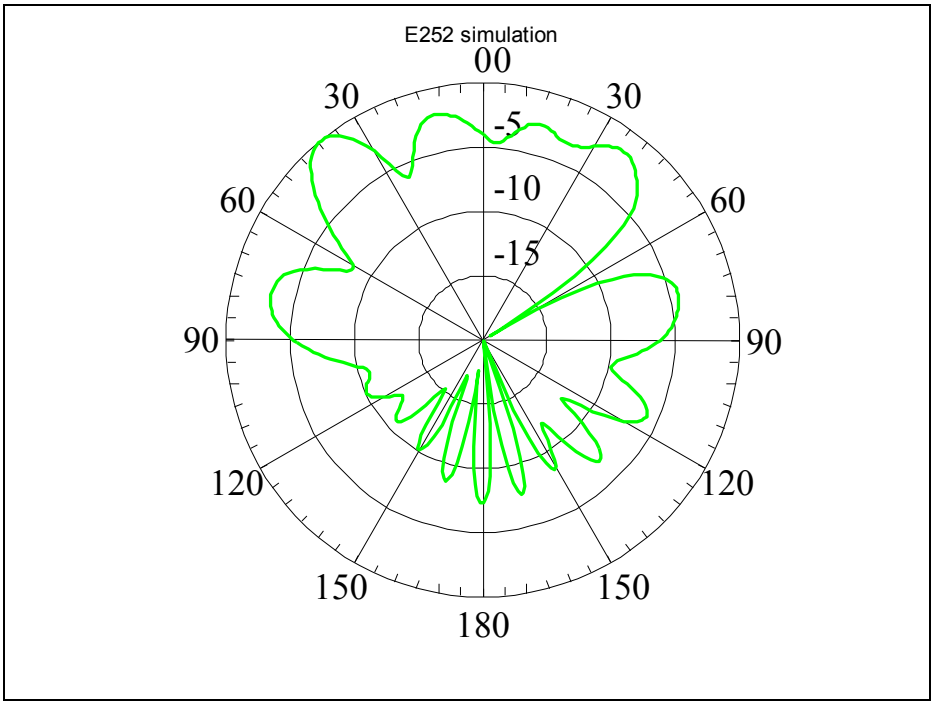

Figure 45 Simulation of Normalized E Plane Pattern at 25.2GHz

5.3.2 Measurement Results of the Patch Antenna

In the laboratory antenna radiation pattern, reflection at the input port (s_{11}), antenna gain and type of polarization can be measured.

S_{11} measurement result which is taken by using network analyzer that gives the reflection from input port for different frequencies is shown in Figure 46. At 24.9 GHz, S_{11} is -33 dBm and at 25.2 GHz it is -13 dBm which means the ratio of reflected power to the input power is 1/20. This result is considered sufficient for matching condition and the other parameter tests are carried out. The frequency shift may be caused by disorders in manufacturing.

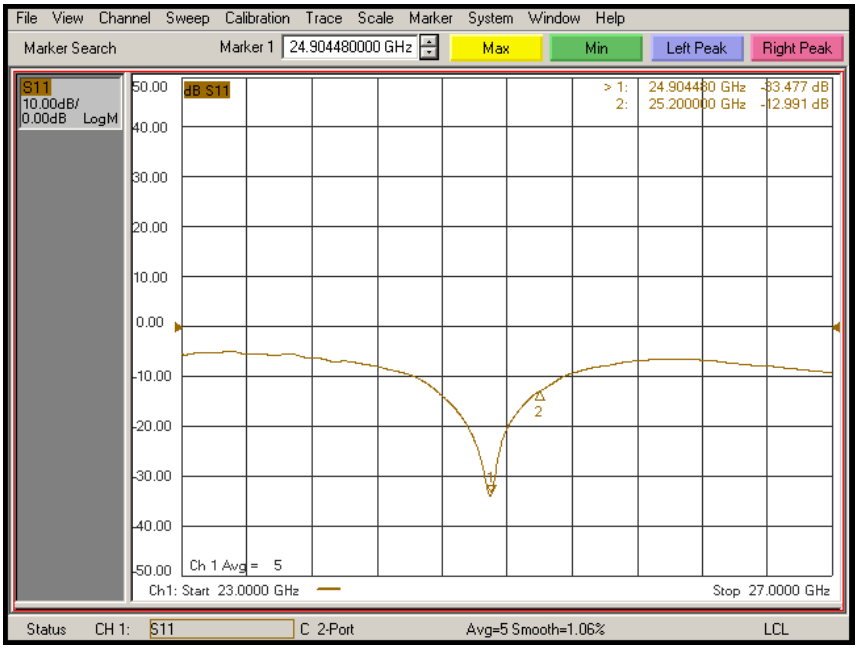

Figure 46 S_{11} Measurement Results of ACMPA

The radiation pattern measurement is performed in an anechoic chamber by using an illumination antenna which can be seen in Figure 47. In the figure the left one is the manufactured aperture coupled microstrip patch antenna and the right one is the horn antenna used for illumination. The measurements are taken by rotating

the antenna in the E plane (yz plane) and in the H plane (xz plane) from 0^o to 360^o for three different frequencies.

For many practical antennas an approximate formula for the gain is used. [19]

$$G_0 = \frac{30000}{\Theta_{1d}.\Theta_{2d}} \qquad \text{(approximately)} \qquad (5.1)$$

Where Θ_{1d}, is the half-power beamwidth in one plane (degrees) and Θ_{2d} is the half-power beamwidth in a plane at a right angle to the other (degrees).

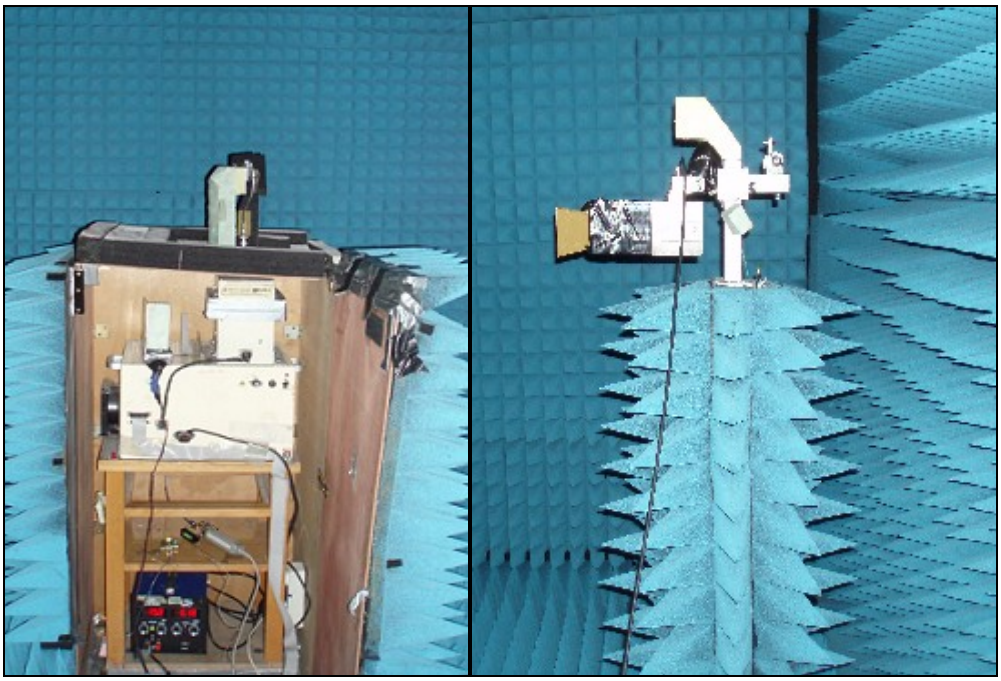

Figure 47 Measurement set up of the ACMPA

The measurements are taken for both directly connecting the microstrip patch antenna to the set up and using absorbers at the edges also on the feed of the

antenna. It is seen that if the absorbers are not used diffraction of the signal from the edges causes distortion on the radiation pattern.

Figure 48 ACMPA Radiation Pattern Measurement with absorbers

The measurement results are taken at 24.8GHz, 24.9GHz and 25.2GHz and then they are normalized and plotted using MATLAB in polar plot and the half power beam widths are calculated for horizontal and vertical planes.

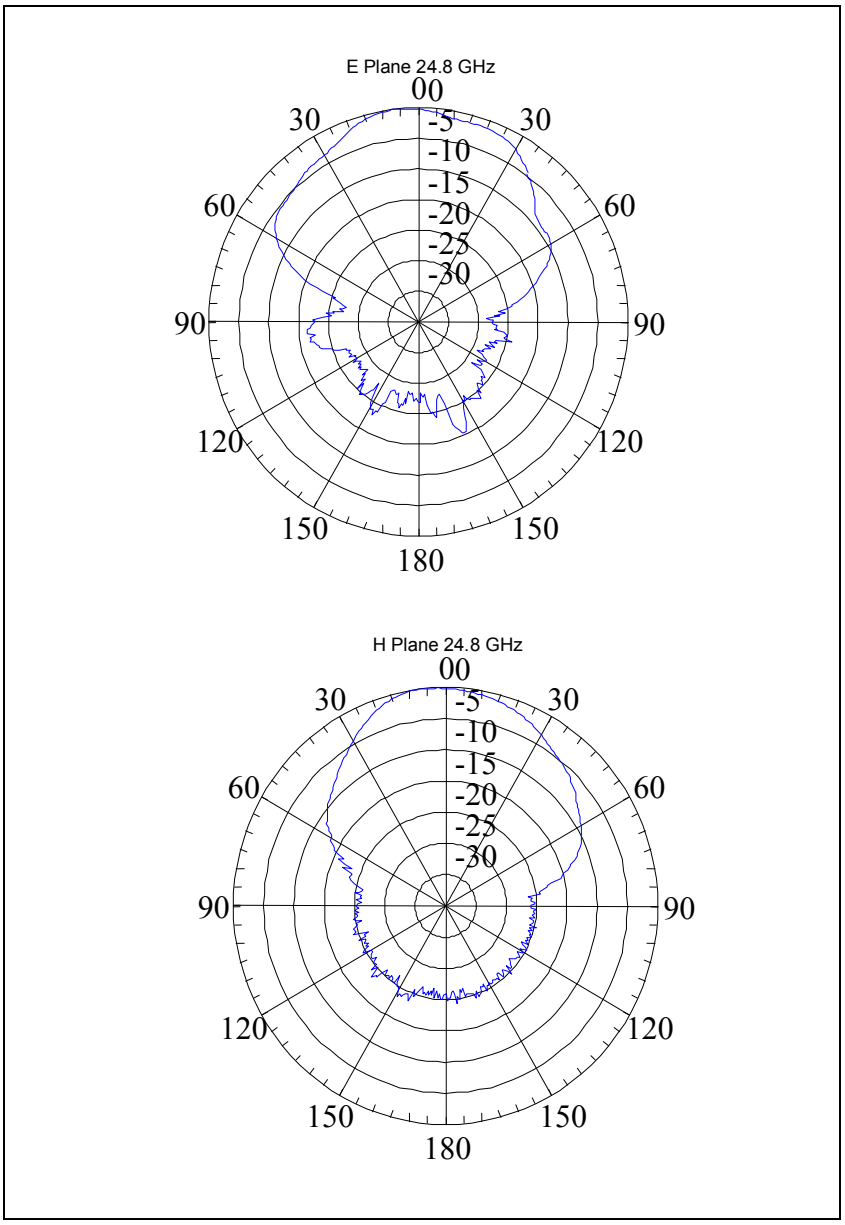

Figure 49 Normalized Radiation Pattern Measurements at 24.8 GHz

Half-power beamwidth in E plane $\Theta_{1d} = 58^{o}$

Half-power beamwidth in H plane $\Theta_{2d} = 52^{o}$

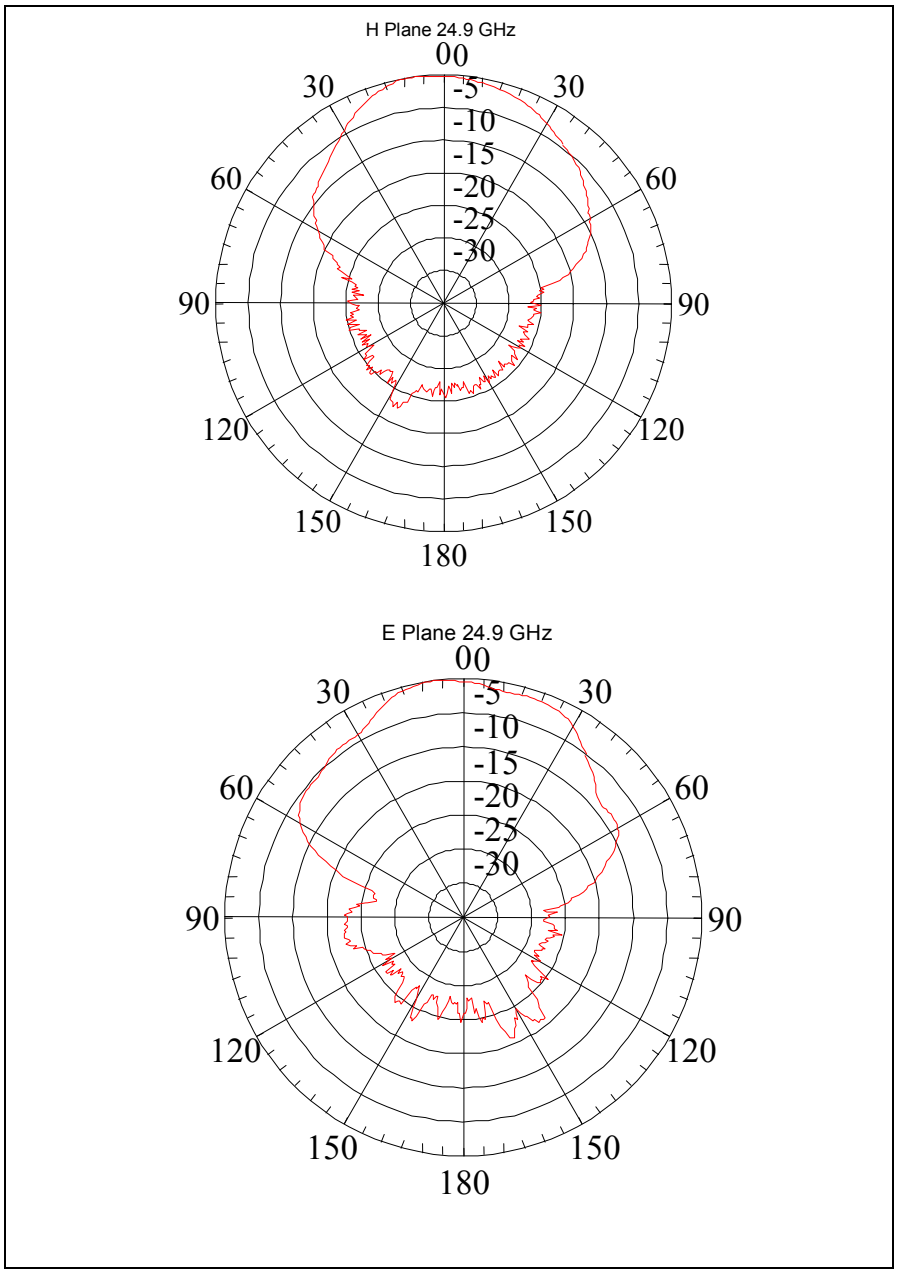

Figure 50 Normalized Radiation Pattern Measurements at 24.9 GHz

Half-power beamwidth in E plane $\Theta_{1d} = 54.8^{o}$

Half-power beamwidth in H plane $\Theta_{2d} = 54^{o}$

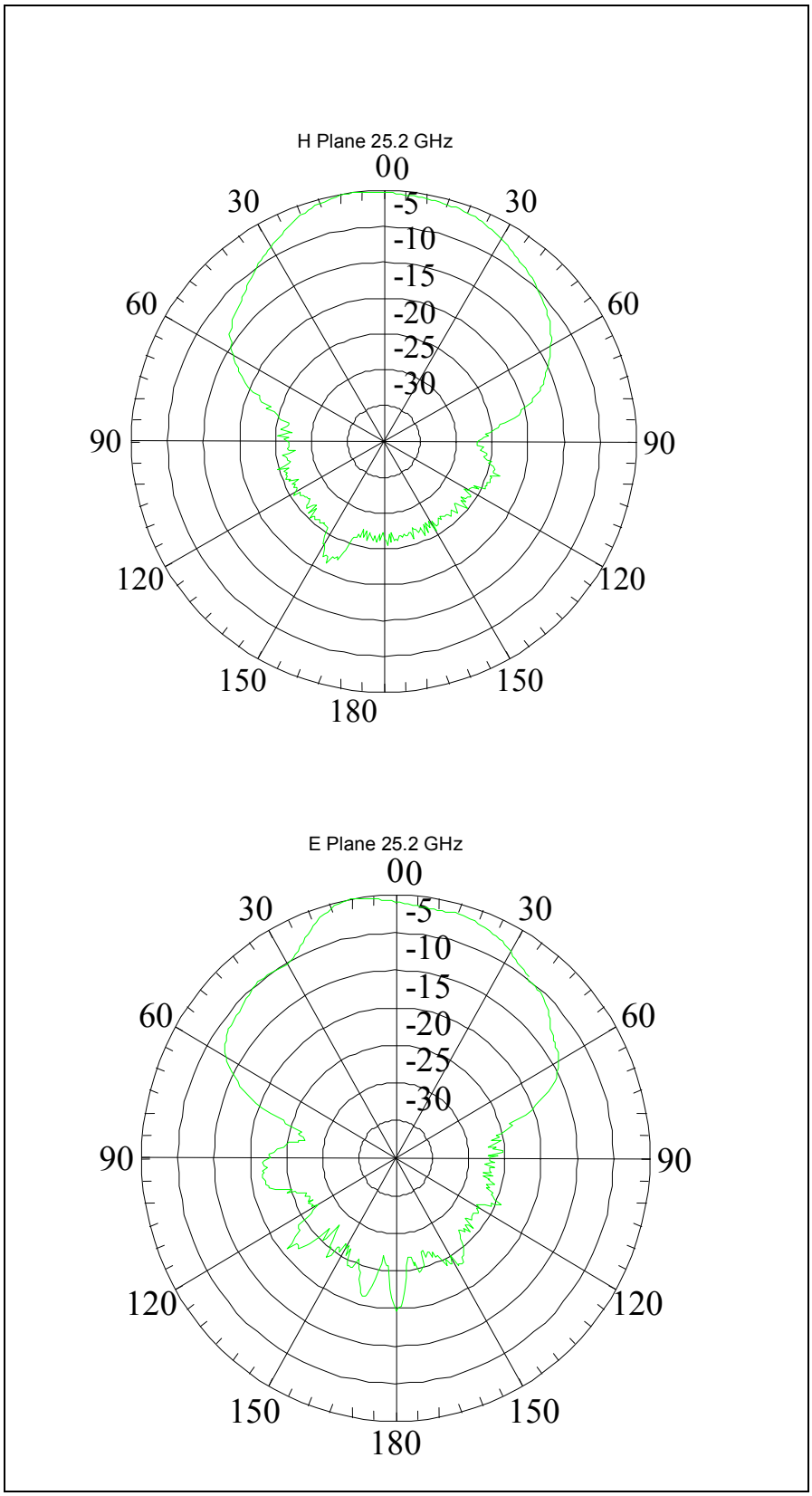

Figure 51 Normalized Radiation Pattern Measurements at 25.2 GHz

Half-power beamwidth in E plane $\Theta_{1d} = 51.9^o$
Half-power beamwidth in H plane $\Theta_{2d} = 60.8^o$

From equation (5.1) the gain of the aperture coupled microstrip patch antenna can be calculated approximately as follows:

$$G(dB)=10\log\frac{30000}{51.9x60.8}=9.7dB \qquad \text{(Approximately)}$$

In conclusion looking at the normalized H field radiation pattern one can say that back lobe radiation cannot be measured because of noise level although E field radiation is more literal for back radiation, hence there may be measurement errors due to absorbers in anechoic chamber.

5.4 Low Pass and High Pass Filters

In this traffic radar system minimum beat frequency is 100 kHz and maximum beat frequency is about 2048 kHz. Hence after mixer to filter beat frequency, first a low pass filter with cutoff frequency of 4 MHZ is used. Then two high pass filters with cutoff frequency of 90 kHz are designed.

Both filters are designed and simulated in FilPRO. For the low pass filter synthesis tool is used. By inserting transmission zeros and optimizing on the return loss and insertion loss graphics, feasible inductor and capacitor values are found which is shown in Figure 52.

Then in the PCAD, circuit scheme is produced and low pass filter is fabricated on FR4 material which has substrate height of 1 mm and dielectric constant of 4.
Then by the same process two high pass filters with 90 kHz cut off are fabricated on FR4 and TMM 10 substrates.

5.4.1 Low Pass Filter Design

In the implementation of the low pass filter surface mount power inductors are chosen because of their low DCR values.

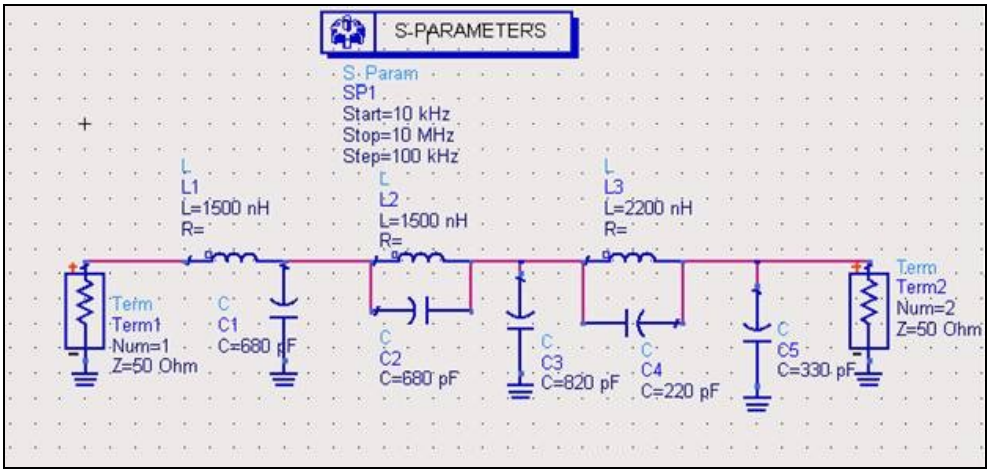

Figure 52 LPF Circuit scheme on ADS

5.4.2 Low Pass Filter Simulation Results

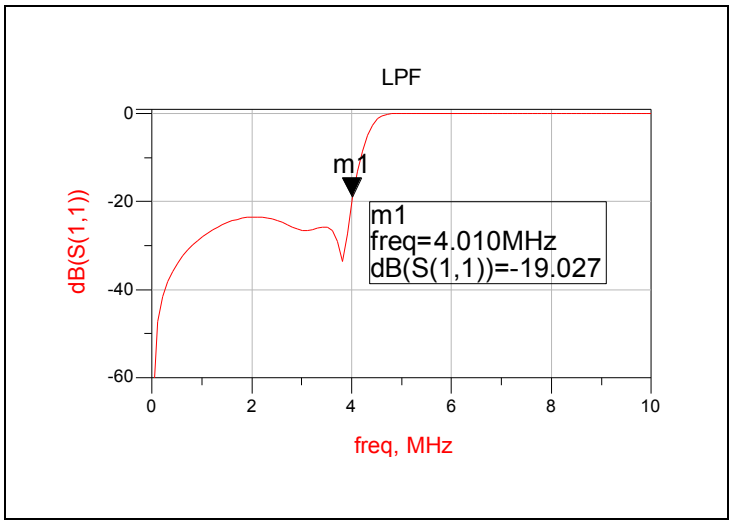

Figure 53 S_{11} (Reflection) vs. Frequency Simulation results in ADS

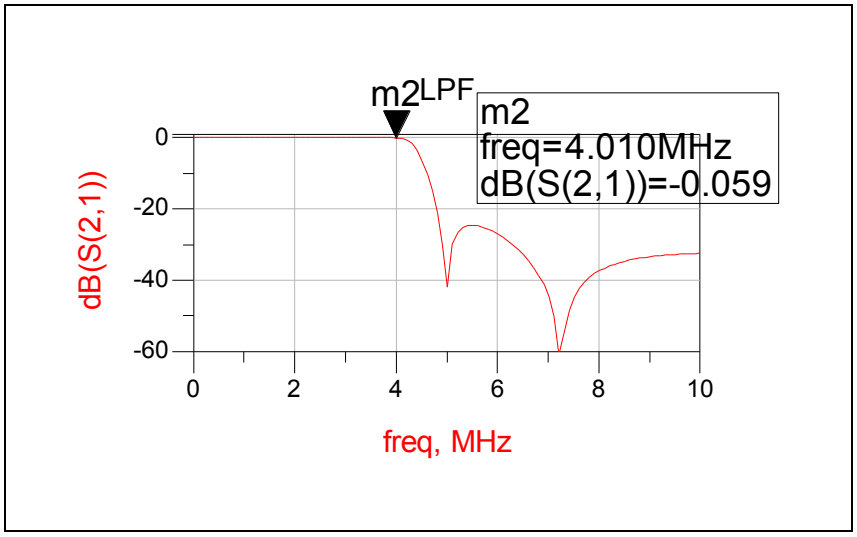

Figure 54 S_{21} vs. Frequency Simulation results in ADS

5.4.3 Low Pass Filter Measurement Results

The characteristic of the filter is obtained by using a signal generator and a spectrum analyzer since the network analyzer does not work in this range. By increasing the signal frequency from 10 KHz to 15 MHz the characteristic of the filter is obtained.

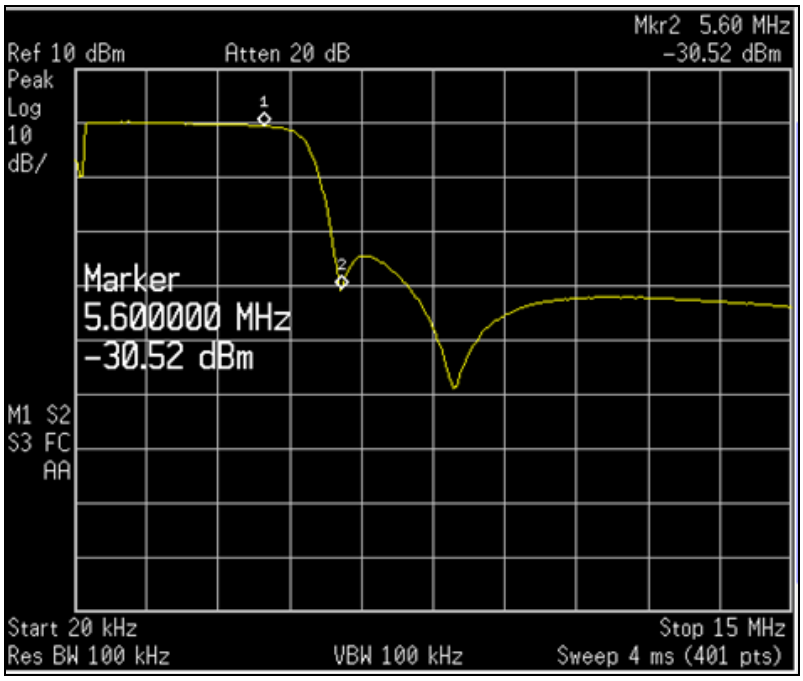

Figure 55 S_{21} Measurement of Low Pass Filter

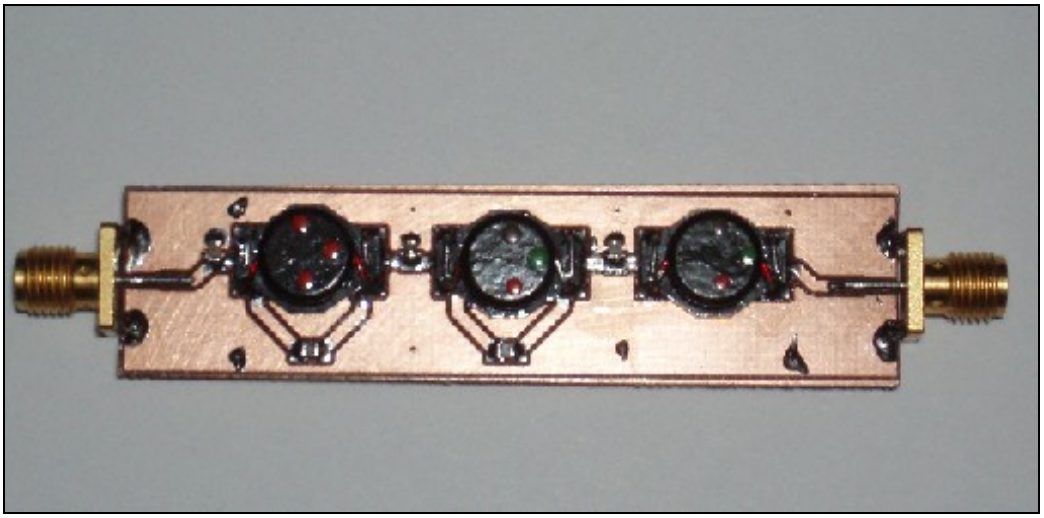

Figure 56 LPF Implementation

5.4.4 High Pass Filter Design

The high pass filter is also designed with synthesis tool in FILPRO and the values are optimized considering S parameters for feasible capacitor and inductor values.

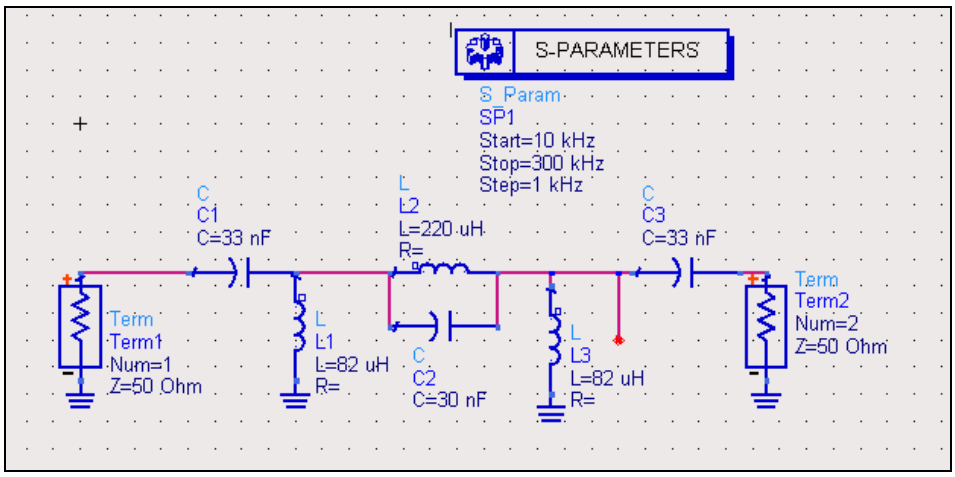

Figure 57 Circuit scheme in ADS

5.4.5 High Pass Filter Simulation Results

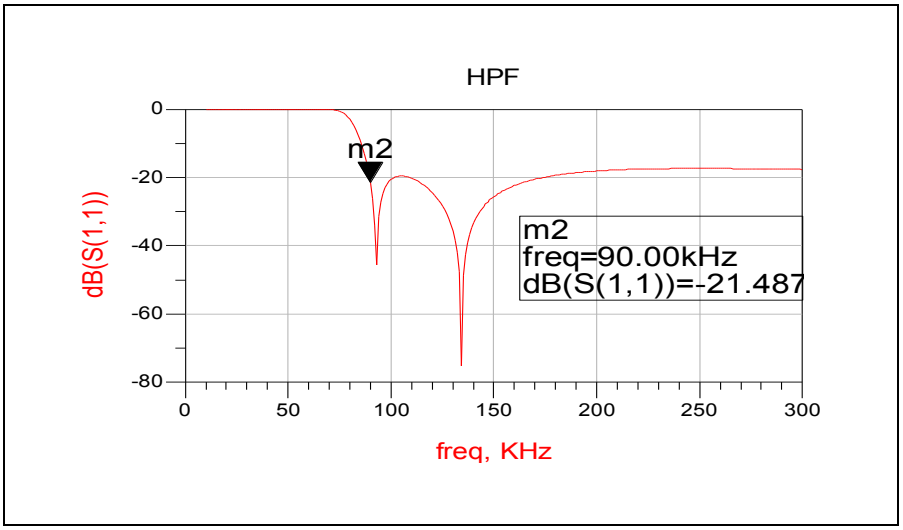

Figure 58 S_{11}(Reflection) vs. Frequency Simulation Result in ADS

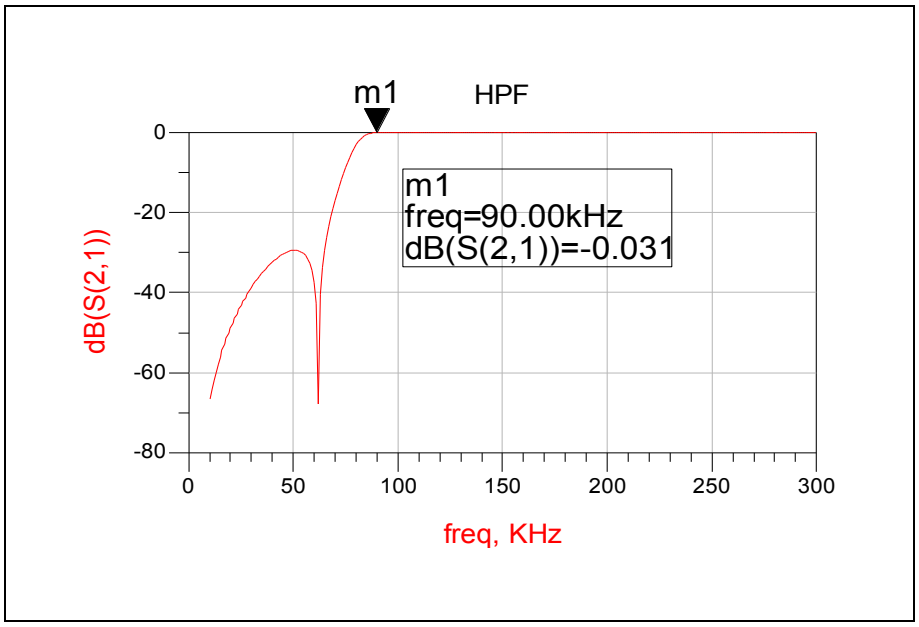

Figure 59 S21 ADS Simulation Results of HPF

5.4.6 HPF Measurement Results

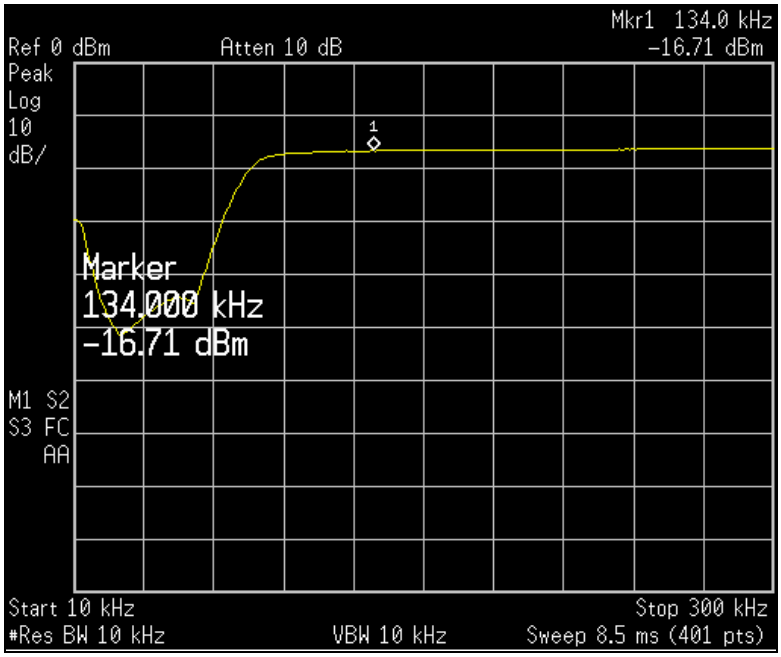

Figure 60 S_{21} Measurement of HPF1

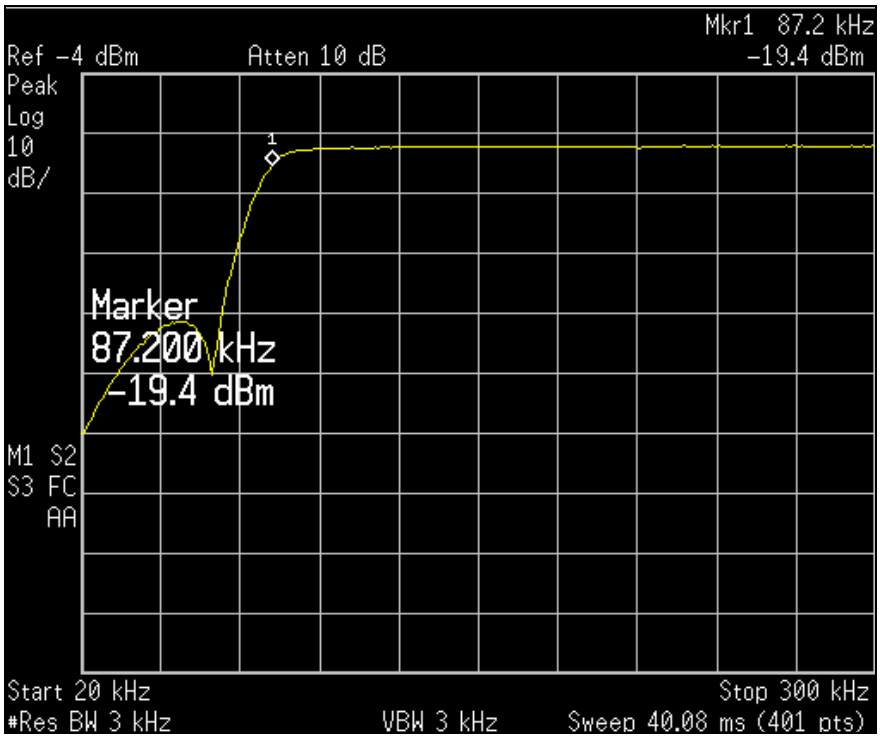

Figure 61 S_{21} Measurement of HPF2

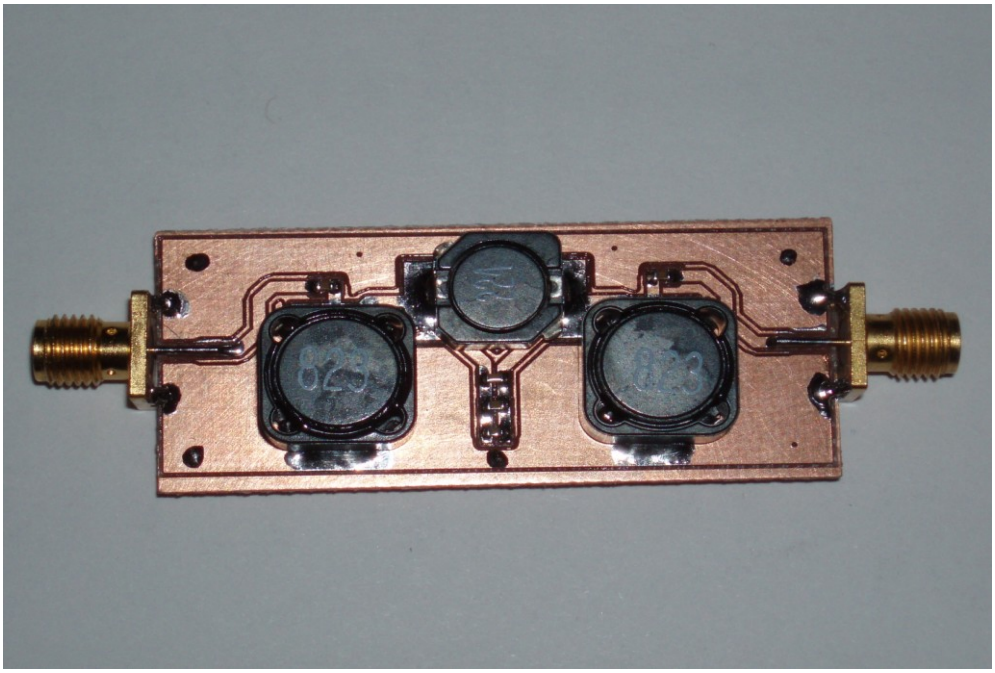

Figure 62 HPF1 Circuit on FR4 Substrate

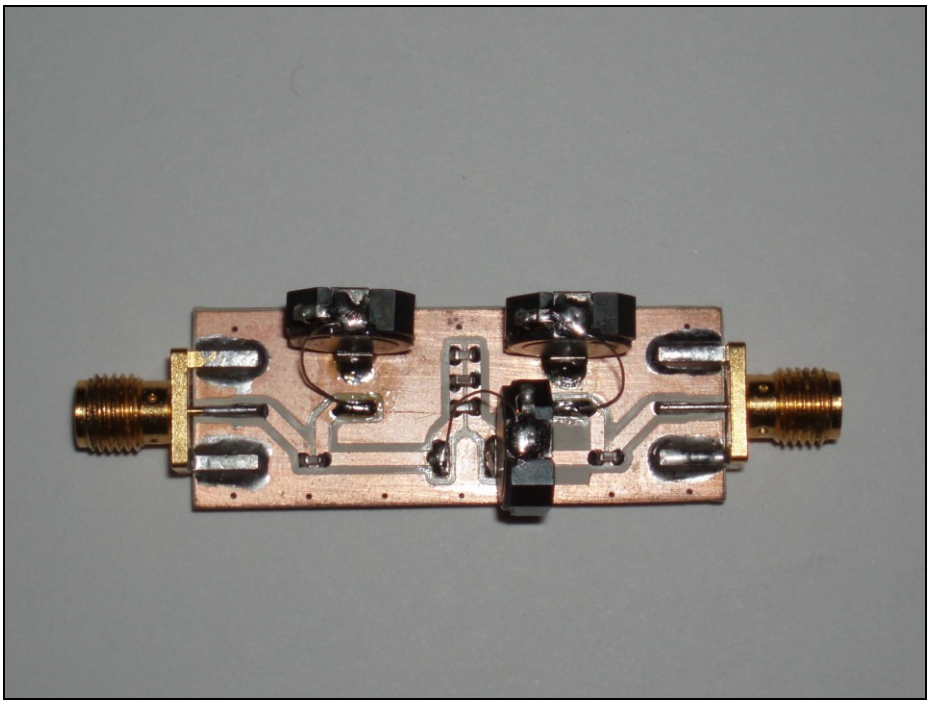

Figure 63 HPF2 Circuit on TMM10 Substrate

The filters simulation results and measurement results are consistent with each other. Since these are low frequencies the inductors are used from surface mount power inductor series whose resistive effects are less in these frequencies.

CHAPTER 6

CONCLUSION

The aim of this thesis is to produce 25 GHz traffic radar using the FMCW method. First of all, general requirements of the traffic radar have been defined, and then circuit design and necessary components have been determined. For the components, the active ones have been procured, while the passive components, which are the coupler, the filters and the antenna, have been designed and manufactured.

In chapter 1, the application areas and the advantages of the FMCW radar are given.

In chapter 2, FMCW radar is described in general, and beat frequency calculation for a moving target is shown.

System requirements, calculation of the system parameters and specifications of the necessary components are described in Chapter 3.

Design, simulation results, manufacturing procedure and measurement results of the 7 dB branch line coupler working at 25.2 GHz are explained in Chapter 4.

In the next chapter, design of the low pass and high pass filters to be used in the system is given. Simulations of the filters as well as the manufacturing steps and measurement results are also included in this chapter. In addition to these, similar explanations are carried out for the aperture coupled microstrip patch antenna.

Throughout the implementation process, the main constraint was getting the suitable components for high frequency the system used.

Available connectors and RF cables do not show the required characteristics above 18 GHz, which have caused problems during the measurement steps.

In the analysis performed with the SMA connectors on a 50 Ohm straight line, it has been found out that these connectors cause a significant reflection for the frequency levels above 10 GHz.

Especially, in coupler manufacturing, 3 different SMA connector structures have been tried but only with 30 GHz connectors it has been possible to operate the coupler. With other structures, S parameters of the isolated and coupled ports have been very close to each other.

Also, the calculated values of the lines are in millimeter and the LPKF router and the router blades used, do not have the necessary precision and sensitivity to meet these millimetric requirements of the PCBs.
Hence in the measurement results of the patch antenna it is seen that maximum radiation is 300 MHz below the design frequency.

The main problematic issue in the filter design is the losses caused by the inductors with small packages and high number of windings. That's why filters have been constructed again with inductors having less winding.

For the VCO HMC533 LP4 tune voltage, a simple addition circuit has been implemented. After that this signal is passed through coupler and high power amplifier and transmit power is measured before the antenna. The measured output power has been below calculated values since the cables used introduce at least 3 dBm loss at this frequency.

To obtain a better linear frequency sweep, tuning voltage of VCO may be pre distorted with a loop system.[20]

For the future works, it is planned to use proper connectors and cables as well as more accurate and sensitive measurement devices. In addition to these, a correction circuit can be used to have a more linear transmit signal. With these improvements, it is planned to develop the system and obtain a proper operation.

REFERENCES

[1]. Skolnik, Merrill I.: Introduction to Radar Systems, McGraw-Hill Book Company, 1980 Second Edition.

[2]. Komarov, Igor V., Smolskiy Sergey M.: Fundamentals of Short Range FM Radar, Artech House, pp 3-9, 2003.

[3]. Stove, A. G.: Linear FMCW Radar Techniques, IEE Proceedings-F, Vol. 139, No. 5, October 1992.

[4]. Toker, C., Saglam, M., Ozme, M., and Gunalp, N.: Branch-Line Couplers Using Unequal Line Lengths, IEEE Transactions on Microwave Theory and Techniques, Vol. 49, No. 4, April 2001.

[5]. Brooker, G.M.: Understanding Millimeter Wave FMCW Radars, International Conference on Sensing and Technology, November 2005.

[6]. Wiltse, C. J., The RF and Microwave Handbook, pp. 172 -180, 2001 Second Edition.

[7]. Barton D., Leanov S., Radar Technology Encyclopedia, pp 256,331-332, Artech in House.1998

[8]. David, W.: Institute of Transportation Studies, California Partners for Advanced Transit and Highways (PATH), FMCW MMW Radar for Automotive Longitudinal Control, 1997

[9]. Secmen M., Demir S., Hizal A.: Dual-polarised T/R Antenna System Suitable for FMCW Altimeter Radar Applications, IEE Proceedings Microwaves Antennas and Propagation, October 2006

[10]. Nathanson, F. E., Reilly, J. P., Radar Design Principles, Review of Radar Range Performance Computations, 1998

[11]. Bayraktar, Ö., Beam Switching Reflectarray with RF MEMS Technology, METU, 2007

[12]. Pozar, M. D.: Microwave Engineering, 2005 Third Edition, pp. 309-336.

[13]. Pozar, M. D.: A Review of Aperture Coupled Microstrip Antennas: History, Operation, Development, and Applications, May 1996.

[14]. Barthia, P., Behl, I., Garg, R., Ittipibon, A.: Microstrip Antenna Design Handbook, 2001, Artech House, pp 2-4.

[15]. Silver, J.P., Micro-strip Patch Antenna Primer RF, RIC & Microwave Theory, Design Retrieved from http://www.zen118213.zen.co.uk/Systems_And_Devices_Files/Patch_Antenna.pdf, August 20,2009

[16]. Wikipedia, The Free Encyclopedia, Proximity Fuze., Retrieved from http://en.wikipedia.org/wiki/Proximity_fuze, July 25, 2009

[17]. Seçmen M., Topallı K., Ünlü M., Erdil E., Çivi Ö., Hızal A., Dual Wideband Antenna Analysis for Linear FMCW Radar Applications, IEEE, 2006

[18]. Hahn, P., Gross, S., Beam Shape Loss and Surveillance Optimization for Pencil Beam Arrays, IEEE Transactions on Aerospace and Electronic Systems, vol. AES-5, issue 4, pp. 674-675

[19]. Balanis C., Antenna Theory Analysis and Design, Wiley, 2nd edition, Ch 14, Ch2, 1997

[20]. Piper O.S., Homodyne FMCW Radar Range Resolution Effects with Sinusoidal Nonlinearities in the Frequency Sweep, IEEE International Radar Conference, 1995

[21]. Hızal, A., "Propagation Aspects of Communication and Radar Systems Lecture Notes", Middle East Technical University/Department of Electrical and Electronics Engineering. 1992-1997, p.44